

Recent Progress in Radiation-Based Investigation Techniques for Understanding Particle Motion—A Review[†]

Tsuo-Feng Wang¹, An-Ni Huang^{2,3}, Wan-Yi Hsu² and Hsiu-Po Kuo^{1*}

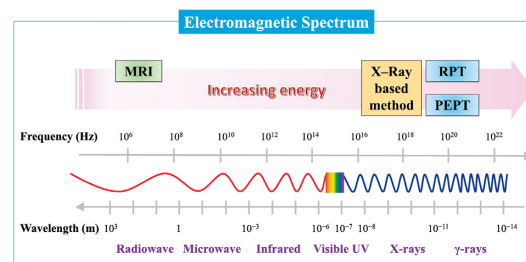
¹ Department of Chemical Engineering, National Taiwan University, Taiwan

² Green Technology Research Center, Chang Gung University, Taiwan

³ Department of Otolaryngology-Head & Neck Surgery, Linkou Chang Gung Memorial Hospital, Taiwan

Particle motion affects microscopic momentum, heat/mass transfers, and macroscopic mixing/separation performances in engineering processes ranging from those involving granular flows to multiphase systems. The primary interests of researchers seeking to improve the performances of such processes are finding the best ways to understand particle motion. Several methods have been developed to understand particle motion, among which radiation-based techniques have shown particular advantages because they can non-invasively investigate dynamic particle motion. This article reviews four prominent radiation-based techniques for studying particle motion, including Radioactive Particle Tracking (RPT), Positron Emission Particle Tracking (PEPT), X-ray-based methods and Magnetic Resonance Imaging (MRI). The principles and characteristics of these techniques are explained, and recent advances and applications are reviewed.

Keywords: non-invasive particle motion investigation, RPT, PEPT, X-ray, MRI



1. Introduction

Particle motion is an important determining factor of the efficiency, yield, and safety of various particle-related industrial processes. This involves the movements of solid substances in continuous phases or dispersed media (gases, liquids, or solids). Such movements determine the mixing and dispersion characteristics of stirred tanks, heat and mass transfer in fluidized beds, and filtration and separation in cyclone separators, to name a few common engineering processes. Consequently, understanding particle motion in continuous phases or dispersion media is crucial for improving the design and operation of industrial equipment and processes.

Techniques for observing and analyzing particle motion can be divided into two main categories: invasive and non-invasive. Invasive techniques use probes or detectors that disrupt the flow field of a system in question. In order to not noticeably interfere with the original flow pattern, the number and size of probes/detectors used for measurement must be minimized, which limits the size of the interrogation volume. Non-invasive techniques are not subject to such limitations and have made significant progress over the past three decades. Earlier non-intrusive techniques,

such as Particle Image Velocimetry (PIV) and Laser Doppler Anemometry (LDA), are only applicable to transparent or near two-dimensional systems, and the volume fraction of tracer particles (or the dispersed phases) usually is below ca. 5 % to avoid scattering-induced measurement errors. Such limitations have greatly hindered the applications of these optically based techniques in particle motion-related processes, where a system of interest (e.g., fluidized beds) often contains a significant amount of solid particles or has a relatively high solid holdup. To overcome these challenges, radiation-based techniques, such as X-ray and γ -ray imaging methods, for studying particle motion have become a popular topic of research. When an X-ray or γ -ray photon interacts with a charged elementary particle (typically an electron), photon scattering occurs and so the energy of the photon decreases and its wavelength increases. When the photon is from the middle energy X-ray or the high energy γ -ray, the photon scattering refers to the Compton effect or electron pair production, respectively. Although the Compton effect and pair production occur at the electron level, photon scattering and photoenergy decreases can be used to identify the photon–electron interaction events on a tracer particle. Radiation-based methods are applicable to both transparent and opaque systems; thus, radiation-based particle motion studies have developed rapidly in recent years.

This review covers four types of radiation-based techniques for investigating particle motion: Radioactive Particle Tracking (RPT), Positron Emission Particle

[†] Received 27 May 2024; Accepted 16 July 2024
J-STAGE Advance published online 1 February 2025

* Corresponding author: Hsiu-Po Kuo;
Add: No. 1, Sec. 4, Roosevelt Road, Taipei 10617, Taiwan
E-mail: hsuipo@ntu.edu.tw
TEL: +886-2-3366-3066 FAX: +886-2-3366-1748

Tracking (PEPT), X-ray-based techniques, and Magnetic Resonance Imaging (MRI). RPT utilizes γ -rays emitted by isotopically labeled tracer particles to track the flow field of a system of interest, which can be single-phase or multi-phase, allowing for accurate mapping of the flow field and determination of the internal dynamics of the system of interest. If γ -rays are generated from the annihilation of electrons and particle-emitted positrons, the particle's position can be determined by the PEPT method. It has been used to successfully measure particle motion in systems such as tumblers and gas–solid fluidized beds. X-rays and electromagnetic waves are also capable of penetrating most materials with minor scattering or absorption. The 3D dynamics of particles in a system of interest can be determined with X-ray stereography, where two consecutive 2D images are captured simultaneously for a desired measurement duration, or X-ray Computed Tomography (CT), where a number of 2D images are captured simultaneously and consecutively throughout the measurement duration. X-ray imaging techniques are particularly suitable for applications requiring identification and localization of specific particles within a granular medium. Nuclear Magnetic Resonance (NMR) spectroscopy has been a widely used analytical technique for over sixty years. It operates by absorbing radio-frequency electromagnetic radiation in a strong magnetic field. NMR spectroscopy is based on the re-orientation of the atomic nuclei of particles or fluids in magnetic fields. Re-orientation is based on the absorption of electromagnetic radiation and depends on the isotopic nature of the particle/fluid nucleus. It is worth noting that the resonance frequency of each nucleus depends on the neighboring chemical environment. Thus, NMR spectra can provide information about the specific functional groups in a sample and the connections between neighboring nuclei in the same molecule. This technique is used to plot information from atomic resonance relaxation (MRI). This review provides an overview of the principles and operational characteristics of RPT, PEPT, X-ray-based imaging techniques, and MRI, as well as a review of recent advancements in particle motion research using these methods.

2. Radioactive Particle Tracking (RPT)

RPT, also known as CARPT (Computer Automated Radioactive Particle Tracking), typically employs an array of scintillation detectors that are sensitive to radiation. These detectors monitor the moving path of each radioactive tracer particle added to the system of interest, thereby obtaining flow-field data within the system. Radioactive nuclides within a particle release excess energy by emitting α -, β -, and γ -rays. α and β particles, which are charged, are readily absorbed by most materials, but highly penetrating γ -rays can travel long distances until they reach a position at which detectors (to record photon counts) are placed.

The detectors are positioned around the container to record the number of photons emitted during the tracer's movement. The recorded photon count primarily depends on the distance between the γ -ray emitter and detector. The detector position is considered as the center of a virtual sphere, with detection distance r as the radius of the sphere, when tracking tracer particles in a fluidized bed, as illustrated in Fig. 1. When the particle is located near the surface of the sphere, the photon count (γ -ray intensity) can be recorded. When the radioactive activity and γ -ray detector's sensitivity are known and multiple detectors (at least three) are used, the position of the tracer particle can be determined via triangulation.

The pioneers of RPT can be traced back to Kondukov et al. (1964), who demonstrated that the motion of solid particles in gas–solid fluidized bed systems could be tracked with the help of radioactive ^{60}Co particles embedded in polypropylene beads. Due to hardware and software limitations at that time, only qualitative results were obtained. In 1985, Lin et al. (1985) successfully performed quantitative measurements of particle motion in fluidized beds using RPT because of advances in both hardware and software capabilities. Continual improvements have ensued over the following years, and many researchers have successfully utilized RPT to investigate the motion of solids and liquids in various systems involving solids, gas–solid, liquid–solid, and gas–liquid–solid phases, such as bubble columns, slurry bubble columns, stirred tanks, gas–solid and gas–liquid fluidized bed systems, and bioreactors, among others. The spatial and temporal resolutions of RPT technology typically lie within the range of millimeters and milliseconds, respectively, providing sufficiently high precision for most practical applications. RPT tracers can be made with a wide range of customizable sizes, shapes, densities, and energies, providing versatility to accommodate different requirements. Unlike the 512 keV γ -rays produced from the annihilation of electrons and positrons in PEPT (as discussed later), the typical energies of the γ -rays emitted by RPT tracers are higher, making RPT

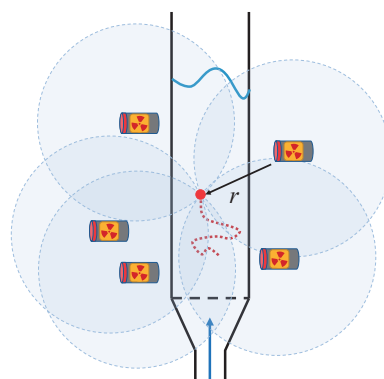


Fig. 1 Schematic diagram illustrating RPT method for locating particle position in a fluidized bed.

well-suited for studying larger and denser systems with photon scattering events. It can detect high holdup and opaque systems, ranging from slowly flowing (almost stagnant) to rapidly flowing (several meters per second) fluid dynamic phenomena. Moreover, RPT is compact compared with PEPT, facilitating its application across various scales of laboratory and industrial setups. This versatility enables *in situ* real-time studies and multifunctionality when detecting different types of multiphase reactors. Nonetheless, RPT requires specialized calibration for the equipment under study. RPT uses high penetration γ -rays, which, unlike easily shielded X-rays, necessitate safety precautions.

Algorithms based on phenomenological or empirical methods are developed to determine the relationship between the recorded photon counts by each detector and the position of the tracer particle. By analyzing the functional relationship between photon counts and tracking time, the time series of the Lagrangian tracer particle positions can be reconstructed. Subsequently, the particle velocity information can be derived from the obtained particle trajectory if the position data acquisition rate is sufficiently high. Fig. 2 represents the RPT concept. However, as the number of traceable particles is practically limited, the amount of information that can be captured within a fixed time is also limited. If one needs to obtain local and global average flow-field data, mixing patterns, and dispersion information, it is typical to use the concept of *ergodicity*. Ergodicity defines a condition in which the representative radioactive particle in a system of interest is monitored at all possible positions. This is typically achieved when the observation time is sufficiently long. Consequently, the trajectory of that single tracer particle over the long observation period should be the same as the trajectories of all particles in the system at any given moment. Theoretically, it has been proven that if the probability of tracer particles visiting all regions is sufficiently high, ergodicity can be safely assumed, provided that the tracer trajectories are recorded over a sufficiently long period of time—to allow tracer particles to pass through the same position multiple times—with sufficient data resolution in each region. Thus, with a sufficiently long observation time, it is possible to reconstruct the residence time or occupancy distributions

in 1D, 2D, or 3D, although requiring longer measurement times. The accuracy of RPT measurements depends on the reliability of reconstructing the positions of tracer particles, that is, to maximize signal sensitivity and resolution. The key factors include detector sensitivity, tracer reactivity, and algorithm. Each of these is briefly introduced below.

2.1 Detector

The detected radiation intensity depends not only on the distance between the radiation source and detector but also on the γ -ray scattering or absorption medium, which causes attenuation. Because the quantity and type of materials in different systems of interest can vary widely, the RPT measurements must be specifically calibrated for each system. If the amount of material between the source and detector varies noticeably over time (such as bubbles in gas-fluidization), it can cause errors in calibration and affect measurements. The calibration procedure involves placing tracer particles at known positions within the system of interest and recording the time-averaged photon counts under *in situ* measurement conditions during a calibration time step. This procedure can minimize errors caused by statistical fluctuations of γ -ray emission and medium attenuation over time.

The configuration array of detectors is critical for accurately reconstructing tracer positions. It is necessary to strategically consider the optimal angles and positions of the detectors. Roy et al. (2002) theoretically modeled the optimal arrangement of detectors. Dubé et al. (2014) advanced this concept by treating the overall resolution of detectors as an objective function. The mesh adaptive direct search (MADS) algorithm was then applied to determine the optimization configuration conditions with the maximized overall resolution. Data sampling frequency also affects the localization accuracy of the RPT. As reported by Kamalanathan et al. (2017), the error in position reconstruction increases with increasing tracer particle velocity and decreases with increasing data acquisition frequency for the same tracer particle velocity. However, at high sampling frequencies, the denominator used in the tracer velocity calculation becomes very small, and even small errors in the position reconstruction can greatly affect the accuracy of the velocity calculation. Thus, it is essential to find the optimal data acquisition frequency for each velocity condition to minimize errors in the position reconstruction and velocity calculation. Lindner et al. (2022) released GIPPE-RPT, an open-source software, for designing RPT experiments. This software allows key RPT parameters to be specified, such as system geometry, materials, the number and types of detectors, as well as types and activities of tracers.

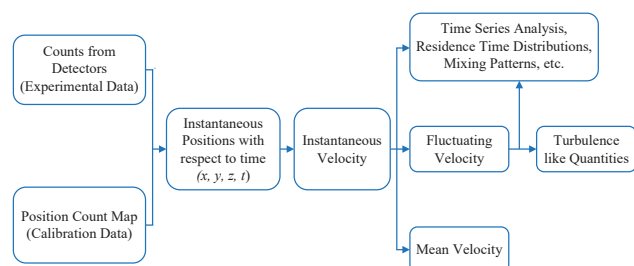


Fig. 2 The concept of the RPT Technology; redrawn based on Yadav et al.'s work (2017).

2.2 Algorithm

Various algorithms have been developed to reconstruct

the trajectories of RPT tracer particles over the past few decades. These include the use of analytical equations typically based on solving a minimization problem (Bhusarapu et al., 2005; Devanathan et al., 1990; Doucet et al., 2008; Mosorov and Abdullah, 2011; Roy et al., 2002; Vieira et al., 2014), Monte Carlo mapping procedures by considering the geometry of the system of interest and the characteristics of attenuating materials (Larachi et al., 1994; Yadav et al., 2017), machine learning models (de Freitas Dam et al., 2019, 2021, 2024; Godfroy et al., 1997; Yadav et al., 2020a), and transfer learning methods (Lindner et al., 2022). A recent study (de Freitas Dam et al., 2024) compared a traditional algorithm developed by Mosorov and Abdullah (2011) with a deep learning model based on a deep neural network (DNN) using data obtained on a simplified model concrete mixer (de Freitas Dam et al., 2021). By comparing the two sets of position mean absolute percentage errors (MAPE) yielded by the two algorithms, the DNN algorithm was more accurate than the traditional algorithm in determining the particle trajectories in the x and y coordinates, and the traditional algorithm performed better in the z coordinate. It is interesting to note that traditional and deep-learning-based algorithm models have their own advantages and disadvantages in terms of position measurement accuracy.

2.3 Tracer

RPT uses a series of carefully arranged detectors to locate the relative intensity of the radiation emitted by radioactively labeled tracers. The accuracy of the RPT particle position calculation strongly depends on the radiation capability of a radioactively labeled tracer to accurately track the phase of interest; therefore, the fabrication of tracer particles with the desired characteristics is crucial. The tracer isotope is typically a γ -ray emitter. As a general rule, tracers made of isotopes emitting higher energy γ -rays are used to image larger, denser systems. Ideally, a tracer should possess physical properties similar to those of the phase being tracked, have a sufficiently long half-life to complete experiments, and should exhibit chemical inertness, thermal stability, and adequate mechanical strength. To track the solid phase/particle phase, the physical characteristics of the particles (such as size, shape, and density) should be similar to those of the solid phase, and the shape of the particles should match that of the solid phase. To track liquid phase flow, tracer particles should follow the liquid phase. Therefore, the particles should be small, wettable spheres with neutral buoyancy (i.e., the density of the particles should be the same as that of the liquid phase). Common tracer radioisotopes for RPT studies include ^{24}Na , ^{46}Sc , ^{60}Co , ^{137}Cs , ^{140}La , ^{192}Ir , and ^{198}Au , which exhibit specific γ energy and half-lives. ^{46}Sc is especially widely used in RPT research due to its neutron cross-section, suitable gamma energy, moderately long half-life,

and flexibility in its production in various chemical forms. Yunos et al. (2014) discussed a simple procedure for preparing radioactive tracer particles. Biswal et al. (2021) discussed the characteristics of radioactive particles used as tracers in RPT experiments and their preparation methods. The sol–gel method and the melt quench in combination with microwave heating are the two most popular methods for preparing customized tracers. These two methods show advantages in producing tracer particles with relatively high specific activity and mechanical strength while minimizing radiation hazards during the preparation process.

Some processes involve particles with different physical properties. For such multiphase systems, separate RPT measurements can be performed to track each phase individually. For example, binary solid multiphase systems have been tested using separate RPT experiments, one for each phase (Roy et al., 2021; Upadhyay and Roy, 2010). The statistical averages of each flow field were then combined to form the flow field of the binary solid mixture. However, tracking each radioactive particle separately may not provide all the necessary information, such as separation and interactions between solid particles. Rasouli et al. (2015) introduced a multiple radioactive particle tracking technique (M-RPT), which tracks the trajectories of two freely moving or constrained (attached to both ends of the same cylindrical particle) tracer particles. By tracking the midpoint of the constrained tracers at both ends of the cylindrical particle, information such as the motion, position, and orientation of the cylindrical particle can be obtained, which is not possible with single-tracer RPT alone. Vesvikar et al. (2023) presented another M-RPT technique that utilized different radioactive tracers with distinct γ energy peaks to simultaneously track the motion of two or more (up to 8) particles with different sizes, shapes, and densities. ^{46}Sc and ^{60}Co were successfully employed to simultaneously track the behavior of solid and liquid phases in three-phase slurry bubble column reactors.

2.4 Recent applications

Scaling up fluidized bed reactors has been the primary research focus for many decades. When conditions in a fluidized bed change, achieving fluid dynamics similarity often involves matching dimensionless numbers, such as Froude and Reynolds numbers, and other dimensionless groups that have developed over time. However, these dimensionless groups are mainly based on global parameters, not the local fluid dynamics. The local fluid dynamics in fluidized bed reactors may change, resulting in different flow patterns and mixing intensities. Efhaima et al. (2017) applied RPT and γ -ray CT techniques to assess the fluidized bed scale-up method based on matching dimensionless groups by measuring local fluid dynamics. They indicated that the above-mentioned dimensionless

Table 1 Recent studies on particle motion in multiphase systems using RPT.

	Type of particle motions studied	Type of operation	System ^a	Tracer
Van der Sande et al. (2024)	Flow pattern; solid circulation; axial dispersion	Horizontal stirred bed reactor	S	Polystyrene beads (¹⁹⁸ Au)
Al-Juwaya et al. (2023)	Residence time distribution; axial RMS particle velocity; particle cycle time; solid eddy diffusivity	Conical-cylindrical spouted bed	G–S	Glass; steel (⁶⁰ Co)
Vesvikar et al. (2023)	Flow pattern; axial velocity	Slurry bubble column reactor	G–L–S	Polypropylene (⁴⁶ Sc and ⁶⁰ Co)
Tribedi et al. (2023)	Axial and radial velocity	Cold-flow riser (bottom section)	G–S	Glass beads (⁴⁶ Sc)
Roy and Roy (2023)	Velocity	Binary fluidized bed	G–S	Spherical bead (⁴⁶ Sc)
Salerno et al. (2022)	Velocity; turbulence level maps	Agitated tank reactor	G–L–S	NaCl (²⁴ Na)
Tribedi et al. (2022)	Velocity; turbulent intensity	Circulating fluidized bed	G–S	Glass beads (⁴⁶ Sc)
Roy et al. (2021)	Velocity	Binary fluidized bed	G–S	Glass beads (⁴⁶ Sc)
Yadav et al. (2020a)	Algorithm comparison	Bubble column	G–L	Polypropylene (⁴⁶ Sc)
Yadav et al. (2020b)	Liquid velocity field	Convective boiling flows	L	Expancel® microspheres (⁴⁶ Sc)
Kalo et al. (2020)	Scale-up	Gas–solid conical fluidized beds	G–S	Glass beads (⁴⁶ Sc)
Patil et al. (2020)	Calibration method; model validation	Stirred tank	L	Plastic ball (⁴⁶ Sc)

^aG: gas; L: liquid; S: solid

groups were not sufficient to represent all local interactions, emphasizing the importance of locally measured fluid dynamics in scale-up evaluations. Ali et al. (2017a) utilized RPT to measure local particle velocities, normal and shear stresses, and turbulent kinetic energy in gas–solid spouted beds to assess the scale-up method proposed by He et al. (1997). Their study also concluded that the above-mentioned dimensionless groups were insufficient to represent all local interactions.

Ali et al. (2017b) used RPT at a sampling frequency of 50 Hz to track gas–solid spouted beds for 6–14 h and evaluated and validated a newly developed mechanistic scale-up methodology. The researchers measured the 3D solid velocity field and turbulent flow parameters. Their experiments confirmed that when the radial profiles of gas holdup matched or closely approximated each other, hydrodynamic similarities were obtained in terms of some dimensionless group values, radial profiles of particle velocities, normal stresses, shear stresses, and turbulent kinetic energy. Matching the radial profiles of gas holdup enabled the successful scale-up of the gas–solid spouted beds. In their subsequent study (Al-Juwaya et al., 2023), RPT was used to measure other solid particle flow parameters in spouted beds to validate the new dimensionless group-based scale-up method. Kalo et al. (2020) used a similar RPT method to validate the Glicksman scale-up method for gas–solid conical fluidized beds.

In reactors, poor solid circulation and inadequate heat dissipation can lead to increased surface temperatures of particles, resulting in the formation of agglomerates or lumps. Van der Sande et al. (2024) used single-photon

emission RPT to investigate flow dynamics, solid circulation, and axial dispersion in laboratory-scale horizontal stirred bed reactors (HSBRs) under different agitating speeds and reactor liquid levels. They found that the solid circulation increased with both the agitator speed and reactor liquid level. The axial dispersion coefficient showed a linear relationship with the agitator speed. Recent research conducted using RPT technology is summarized in Table 1.

3. Positron Emission Particle Tracking (PEPT)

Positron Emission Tomography (PET) is a widely used medical imaging technique that provides unique information about the body to physicians in hospitals. Unlike CT or MRI, which primarily examine anatomical structures, PET enables visualization of body function. PET imaging requires access to a cyclotron that produces *positron-emitting* radioisotopes (nuclide or isotope), like ¹¹C, ¹³N, ¹⁵O, or ¹⁸F. These cyclotron-prepared positron-emitting radioisotopes are incorporated into other chemical compounds, including normal body components, like oxygen (used to image blood flow) or drugs (used to visualize brain chemical systems), to make radiopharmaceuticals. When a positron annihilates with an electron, collinear back-to-back γ -rays are produced and detected by a scanner. Collinear back-to-back γ -rays, which are a pair of γ -rays that are emitted simultaneously in exactly opposite directions (180 degrees apart) along the same straight line, are schematically shown as yellow lines in Fig. 3. The scanner contains rings of scintillation detectors, whose electronics process their signals to create mapping images of the sampled volume

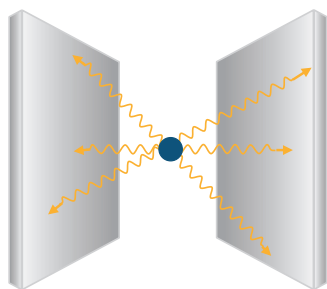


Fig. 3 Schematic diagram illustrating PEPT method for locating particles by γ -ray pairs.

containing radiopharmaceuticals. Because the radioisotope used in PET is short-lived, the patient's radiation exposure is usually small. Nevertheless, a substantial amount of data is required to achieve a reasonable signal-to-noise ratio in PET measurements, which takes a long time. Consequently, changes occurring within a very short timeframe are difficult to detect. To counter this difficulty, Positron Emission Particle Tracking (PEPT) technology was developed in the late 1980s at the University of Birmingham, UK, which enables the tracking of the rapid movements of individual tracer particles to determine their 3D dynamic behaviors without interrupting the process of interest. PET and PEPT both use the principles of positron emission and annihilation, but their reconstruction methods are different. PET provides detailed images of the distribution and concentration of tracers, requiring high spatial resolution and sensitivity for imaging. PEPT is used for tracking the position, velocity, and trajectory of labeled tracers in real time, requiring high-time resolution to accurately track and analyze particle dynamics.

When a radioactive nuclide tracer is introduced into a system of interest by PEPT, the unstable nuclides will undergo a β -decay. This decay transforms a proton into a neutron (n), positron (e^+), and neutrino (ν):



Positrons (e^+) emitted from tracers may undergo annihilation with local electrons (e^-), producing a pair of back-to-back 511 keV γ -rays, with trajectories separated by $180^\circ \pm 0.5^\circ$:



The distance traveled by a positron before annihilation is inversely proportional to the density of the medium. Although positrons do not travel in straight lines, their travel distance is often short because the emitted positron's energy is much lower than the maximum emission energy. Therefore, in relatively dense media, it is reasonable to use the positron's position to represent the location of the tracer in any solid or liquid medium.

Based on the conservation of momentum, each pair of generated γ -rays possesses equal energy but opposite prop-

agation directions. These γ -rays are highly penetrating and propagate along straight lines, with an annihilation event occurring at the midpoint of this line. A coincidence event where two detectors simultaneously detect the γ -rays emitted by the tracer within 25 nanoseconds produces a line of response (LOR). Because only one radioactive tracer is introduced into the system (in most studies), collinear pairs detected multiple times per second should intersect each other, as illustrated in Fig. 3. A pair of detectors records the coincidence events, and the coordinates of the events and times of arrival are stored event-by-event on the computer. If sufficient signals are obtained and the true signals can be distinguished from the noise, the position of the tracer can be reconstructed using the recorded events and triangulation method. The history of the location of the tracer particle can be recorded in three dimensions as a function of time.

The high penetration γ -rays enable the tracking of particle motion in large, dense, and optically opaque systems with high temporal and spatial resolutions theoretically down to microseconds and micrometers, respectively. Currently, full three-dimensional tracking of one or multiple tracers in a given system is achievable. However, in situations with high particle velocities (>1 m/s), short residence times (requiring extensive recirculation or tracking of multiple particles), and small particle sizes (low activity), tracking efficiency is lower, making it challenging to collect statistically significant data. PEPT data typically include positional information of tracer particles as a function of time in the x , y , and z directions. Supplementary devices can be used to record additional information in parallel with the tracer trajectory data. For instance, radioactive labels can be attached at specific locations, such as the tip of the blade or the central joint plane of a V-blender, and sufficient data can be collected to locate physical boundaries. The space within the container can be further divided into volume elements or voxels, and the residence time and average velocity of the tracer particles in each voxel can then be analyzed.

Over the past four decades, the PEPT operation, tracers, algorithms, software, and hardware have evolved and improved. The latest developments in PEPT have focused on developing algorithms to reconstruct trajectories using multiple tracers simultaneously and designing novel modular detector systems. In particular, in the last decade, algorithmic advancements using technologies such as machine learning have made significant progress. [Windows-Yule et al. \(2022\)](#) recently published a comprehensive review of PEPT technologies and their applications. An overview of the key factors influencing the accuracy of the PEPT measurements, including the tracer, detector, and algorithm is reviewed.

3.1 Detector

Early positron-detection systems developed by Rutherford Appleton Laboratory (RAL) in the late 1980s used multi-wire technology to detect γ -rays, offering high resolution. However, as only 7 % of γ -rays hitting the detector were detected, the maximum efficiency at the center was only 0.5 % of all the annihilation events (0.07×0.07). Although this lower detection efficiency is unsuitable for medical purposes, its high-resolution capability has attracted the interest of engineers. Because it is not intended for medical use, the exposure time and/or radionuclide inventory can be increased to provide sufficient statistical data to distinguish real signals from background noise in the resulting images. The original RAL positron camera could locate tracers moving at 1 m/s with a displacement of approximately 5 mm, occurring approximately 50 times per second. The main limitations of the proposed method are its low sensitivity and corresponding low data acquisition rate. Moreover, its uncertainty in particle position was anisotropic: the uncertainty in the direction normal to the detector face was approximately 2.5 times larger than that in the other directions. To enhance the capability of PEPT technology, the aims are typically to increase data acquisition rates and reduce the dead-time factors of positron detectors. The Birmingham ADAC Forté Camera, installed in 1999, offered higher data rates because it was equipped with two scintillation detectors. The main feature of this gamma camera is its high count rate of up to 200 kcps (Forster et al., 2000), which can distinguish very fast pulses and partially process signals from different regions of the crystal simultaneously. The dead time per pulse is approximately 170 ns, and each head can operate at a single rate of over 2 Mcps. With more events detected per unit time, the coincidence resolution time was reduced to 7.5 ns, resulting in a smaller proportion of misleading signals. The useful count rate is over 100k events/s, representing a data rate increase of around 20 to 40 times compared to the RAL camera with better resolution (down to ca. 200 μ m). The detectors are also mounted on a motorized gantry that can rotate around a horizontal axis and adjust the face-to-face spacing between 250 and 800 mm. This approach is more flexible than traditional analog circuits and produces less distortion near the edges of the scintillating crystal of the

scintillation detector. Another PEPT facility was established in PEPT Cape Town (iThemba LABS, South Africa) in 2009 and was capable of tracking tracer particles moving at speeds of up to 10 m/s with a location uncertainty of less than 1 mm.

PEPT can use various *modular* camera systems for different systems as needed (Burnard et al., 2014; Ingram et al., 2007; Leadbeater and Parker, 2011; Sovechles et al., 2017). Modular cameras consist of a set of individual detectors that can be arranged around the equipment in any configuration suitable for particle tracking. Because the detectors can be placed individually around the system, they allow for studying systems of considerable size. Recently, developments in PEPT have focused more on the configurations of modular camera systems. These modular PEPT cameras enable *in situ* studies of the dynamics of larger equipment, broadening the utility of PEPT. Sixteen ECAT951 modular cameras were utilized to successfully track low-activity and high-speed particles, achieving the successful tracking of <500 μ m sized quartz particles in a cyclone reactor (Sovechles et al., 2017).

3.2 Tracer

PEPT tracers are typically prepared from particles of interest and cyclotron activated as the positron emitter; thus, the physical properties of the tracers are mostly identical to those of the particles of interest. Tracers are usually produced using three methods: direct activation, ion exchange,

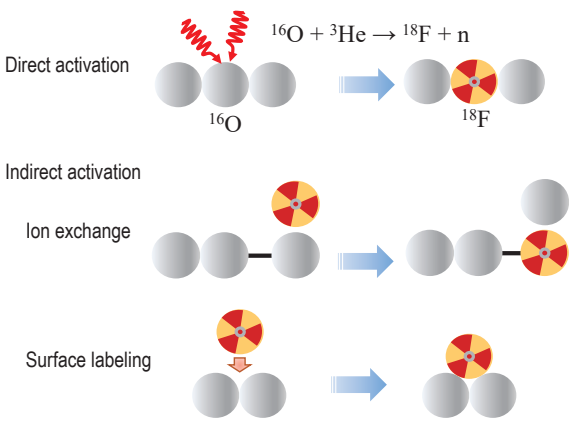


Fig. 4 Schematic drawings of the PEPT radioactive tracer labeling methods.

Table 2 Methods of PEPT tracer particle preparation.

Direct activation	Indirect activation	
	Ion exchange	Surface labeling
Activate existing atoms via ion beam irradiation	Remove the atoms from the material and replace them with a positron emitter	Adhere a radioactive isotope onto existing atoms
<ul style="list-style-type: none"> Suitable for large particles (>1 mm) and high melting point particles Good radiochemical stability 	<ul style="list-style-type: none"> Easy process Low radiochemical stability 	<ul style="list-style-type: none"> Applicable to many inorganic particles

and surface labeling, as summarized in **Fig. 4** and **Table 2** (Fan et al., 2006; Windows-Yule et al., 2022). The isotopes commonly used for medical PET tracers are ^{11}C , ^{13}N , ^{15}O , and ^{18}F , and PEPT tracers typically use ^{18}F or ^{68}Ga . As an example of the direct activation method, ^{18}F -containing tracers are prepared from oxygen-containing particles of interest using cyclotron irradiation through the following reaction:



Leadbeater et al. (2024) recently reviewed the manufacturing techniques for PEPT tracer particles and introduced a direct activation method using high-energy alpha particle beams. Recent developments in tracer fabrication have focused on developing small, biocompatible tracers to expand the application of PEPT to biomedical areas.

3.3 Algorithm

The fundamental PEPT algorithm remains largely unchanged from its initial implementation, known as the Birmingham method, which minimizes the root mean square distance to the Minimum Distance Point (MDP) to remove false coincidences and iteratively calculates new MDPs. This method requires a number of Lines of Response (LoRs), typically on the order of 100. The measurement errors in tracer positions arise from several factors: (1) too long “positron flight” (i.e., the distance traveled by positrons between positron emission and annihilation); (2) the finite spatial resolution of the detectors; (3) detection of “false coincidences”, where not all LoRs correspond to true annihilation events, as examples shown in **Fig. 5**.

Several algorithms have been developed to improve the positional accuracy for both PEPT and PET (Windows-Yule

et al., 2022), particularly the growing demand for PET for tracking moving cells. Lee et al. (2014) reconstructed the time-varying positions of individual radiolabeled moving cells directly from PET measurements using an efficient trajectory reconstruction algorithm. The authors claimed that the algorithm could track a single moving cell within a small animal PET system with 3 mm accuracy. The algorithm selection depends on the system of interest and research objectives. There appears to be no single best algorithm. The number of particles simultaneously tracked increased to over 100 over these years, although the accuracy decreased with the introduction of more tracers (Mandel, 2020; Nicuşan and Windows-Yule, 2020; Wiggins et al., 2016; Yang et al., 2006, 2007). The feature point identification method, in particular, can process signals from at least 100 tracers (Wiggins et al., 2017). Novel algorithms using machine-learning-based clustering techniques have also been used to locate and track several PEPT tracers (Mandel, 2020; Nicuşan and Windows-Yule, 2020) that are capable of tracking at least 128 tracers.

3.4 Recent applications

Early PET and PEPT studies were primarily conducted for high-precision imaging of large, opaque, and rapidly moving equipment systems, including studies on the global mixing and separation of large numbers of particles. Hawkesworth et al. (1986) employed 2D PET to study the fluid dynamics of aircraft engines. Broadbent et al. (1993) investigated batch multiblade mixers under different operating conditions. Fangary et al. (2000) used buoyant tracers to monitor the flow field of viscous non-Newtonian fluids in stirred tanks. PEPT was later used to understand the fundamental phenomena and dynamics underlying particle mixing and separation. Parker et al. (1997) examined particle motions in rotating drums and separately studied radial and axial motions. Stein et al. (2000) studied particle behavior in fluidized beds. Kuo et al. (2002, 2003, 2004, 2005) used millimeter glass bead tracers to obtain the flow patterns in V-blenders and bladed mixers. Wildman and Huntley (2002) examined particle trajectories in a vibrated granular bed, obtaining information about the evolution of displacement density, granular temperature, packing fraction, and diffusion coefficient. Until now, PEPT has been successfully applied to various process equipment to characterize particle flow fields, including fluidized beds (Laverman et al., 2012), stirred mills (Jayasundara et al., 2011), tumbling mills (Govender et al., 2013; Tupper et al., 2016), rotating drums (Morrison et al., 2016; Windows-Yule et al., 2017), mixers (Guida et al., 2009; Kuo et al., 2005), stirred tanks (Windows-Yule et al., 2020), and more challenging unit operations, such as hydrocyclones (Radman et al., 2014; Sovechles et al., 2017), spiral concentrators (Boucher et al., 2016), and flotation cells (Cole et al., 2014).

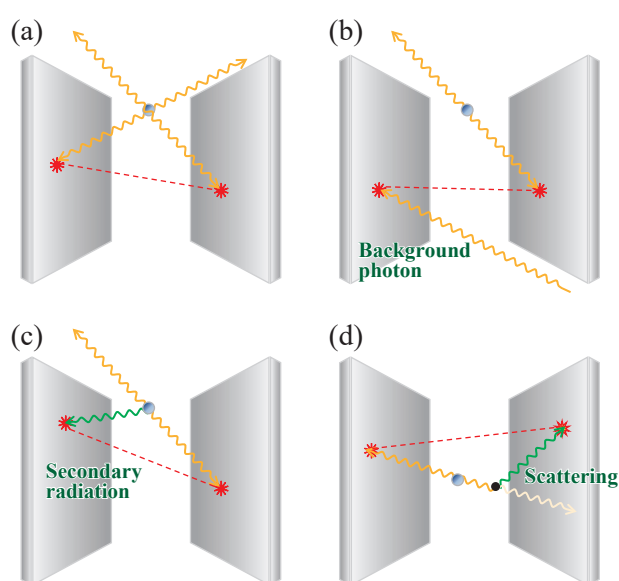


Fig. 5 Possible false coincidence LoRs: (a) random coincidences type I; (b) random coincidences type II; (c) associated coincidences; (d) scattered coincidence; redrawn based on Windows-Yule et al. (2022).

Table 3 Recent studies on particle–liquid motion in multiphase systems using PEPT.

	Type of particle motions studied	Type of operation	System ^a	Tracer
Hart-Villamil et al. (2024)	Model validation	Horizontal laminar stirred tank (Plowshare mixer)	L	Newtonian glycerol
Savari et al. (2024)	Comparison of experimental technologies	Horizontal particle–liquid pipe flow	L–S	Nylon-66 particles in water
Mittal et al. (2024)	Model validation	Tumbling mill	L–S	Slurry
Al-Shemmeri et al. (2023)	Occupancy and velocity measurements	Rotating drum	S	Coffee bean
Che et al. (2023a)	Model validation	Spouted bed	G–S	Coffee bean; cannellini beans; jasmine rice; popping corn; pearl barley
Leadbeater et al. (2023)	Trajectory and velocity measurements	Fluidized bed	G–S	Silica sand; fluid cracking catalyst (FCC)
Che et al. (2023b)	Model validation	Bubbling fluidized bed	G–S	Silica sand
Jones-Salkey et al. (2023)	Trajectory and mixing behavior measurements	Incline linear blender	S	Microcrystalline cellulose
Zhou et al. (2023)	Separation mechanisms	Fluidized bed	G–S	Quartz; hematite
Richter et al. (2023)	Location probability and velocity distribution measurements; model validation	Cyclone	L–S	Coal particles
Cole et al. (2022b)	Velocity distribution measurement	Stirred tank reactor	G–L–S	Silica
Mesa et al. (2022)	Velocity distribution measurement	Flotation tank	G–L–S	Hydrophobic and hydrophilic resin bead; alginate hydrogel
Moodley et al. (2022)	Model validation	Rotating drum	S	Glass bead
Mesa et al. (2021)	Occupancy and velocity measurements	Flotation cell	G–L–S	Hydrophobic and hydrophilic resin beads
Al-Shemmeri et al. (2021)	Occupancy and velocity measurements	Spouted bed	G–S	Coffee bean

^aG: gas; L: liquid; S: solid

Guida et al. (2010) suspended coarse glass particles at concentrations of up to 40 wt% in water, creating an opaque dense slurry. They selectively labeled glass particles (solid phase) and buoyant resin tracers (fluid phase) using direct irradiation to track the solid and liquid phases separately. This allowed them to measure the flow fields, complete 3D velocities, and concentration fields of both liquid and solid phases. Tupper et al. (2016) used high-concentration solid slurries (30 wt%) but with smaller tracer particles (ca. 500 μm), reflecting the behavior of fluids in real grinding mills. Windows-Yule et al. (2017) simultaneously used glass (^{18}F) and steel (^{55}Co) bead tracers to investigate the effect of internal geometry on segregation in binary particle systems. Particles of the same size but different densities exhibit limited, localized axial segregation due to the end-wall effects (Huang et al., 2013; Kuo et al., 2016; Huang et al., 2021a, 2021b). The Cape Town team in South Africa has used PEPT to measure the motion of tracer particles in flow systems such as mineral froth flotation (Cole et al., 2022a). The tracers were coated differently to simulate the hydrophobicity and size of the

minerals. The PEPT experimental results are heavily used to validate the discrete element method (DEM) simulation predictions for the corresponding vessels (González et al., 2015).

The use of PEPT is relatively expensive, and its algorithms are complex. Researchers have used numerical modeling to simulate PEPT hardware and experiments, thereby creating artificial PEPT data from simulated fluid flows (Herald et al., 2018, 2021; Langford et al., 2016). The feasibility of PEPT experiments in a given experimental system can be tested in advance, thereby avoiding unnecessary testing and/or failed experiments. In contrast, real-time data from PEPT were used to validate the artificial PEPT model's output (Windows-Yule et al., 2016). Table 3 summarizes recent studies on particle motion using PEPT techniques.

4. X-ray method

A variety of X-ray imaging techniques have been used for analyzing particle motion. X-rays penetrate most materials with different degrees of attenuation, and X-ray

attenuation maps are analyzed to reveal information about systems containing particles, such as information on the size, distribution, and porosity of the particles (Lin et al. 1992; Yates et al., 2002; Zhou et al., 2021). If one can dynamically acquire X-ray images as a function of time, the temporal evolution of particle motion can be obtained. The main advantages of using X-ray imaging for particle motion characterization are that it does not require radioactively labeled tracer particles or expensive detectors. Nevertheless, the use of ionizing radiation still requires safety shielding of the measurement system. Recent artificial intelligence models have demonstrated the ability to collect time-series X-ray mapping images and analyze particle motion in a more convenient manner. In this study, three X-ray imaging techniques, X-ray radiography, X-ray stereography, and X-ray computed tomography (CT) were reviewed.

4.1 X-ray radiography

The principle of X-ray radiography is graphically illustrated in Fig. 6. The contrast, clarity, and sharpness of images obtained by X-ray radiography are influenced by the sample material, X-ray energy, X-ray scattering, beam hardening, and other settings, which must be carefully adjusted to obtain optimal results. Typical X-ray radiography enables rapid acquisition of images with spatial and temporal resolutions ranging from 0.1 to 0.3 mm and 0.05 to 3 ms. By reducing the field of view, spatial and temporal resolutions can potentially reach values as low as 400 nm and 40 ms (Errigo et al., 2023a).

When using X-ray radiography, the tracer particles require sufficient X-ray attenuation contrast against other materials in the analyzed system. Tracer particles with significantly different densities from those of the particles of interest may be easier to trace because of their higher attenuation contrasts, but they may not accurately represent the trajectories of the particles of interest. To characterize the dynamics of particles within a system representatively, the tracer particles must resemble the particles of interest in terms of size, shape, and density. Accordingly, tracer particles are often required to verify their following efficiency, which is defined as the efficiency of a tracer particle in accurately following the trajectories of the particles of interest.

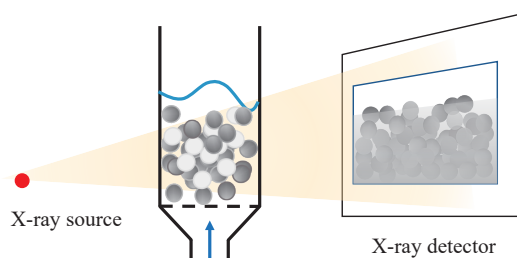


Fig. 6 The operating principle of analyzing particle motion in a fluidized bed using X-ray radiography.

est. Uchida and Okamoto (2006) used tungsten metal particles, which had higher densities than their particles of interest, as tracers to study particle trajectories in a spiral mixer. They reported that when the density of the tracer particles was less than 20 times that of the particles of interest, no noticeable differences in tracer tracking were observed. A common practice to tailor the effective density of a tracer is to use a combination of high-density materials (e.g., metals) with low-density materials (e.g., polymers) to fabricate the tracer, with the goal of matching the tracer density to that of the particles of interest (Nadeem et al., 2023a). Yang and Fu (2004) soaked low molecular weight microcrystalline cellulose Celphre™ particles in a 0.5 M lead (II) acetate solution, and used the Pb-cellulose composite tracer to study particle motion in a V-blender. Kingston et al. (2015) soaked red oak chips in a potassium iodide solution and then coated their outer surface with five layers of silver paint to create tracers with high X-ray absorbance. Parker et al. (2022) developed 50 μm tungsten-coated hollow carbon spheres for use as tracers. Compared to the silver-coated tracer particles, the tungsten-coated tracer particles improved the contrast, making the coated tracer particles easier to locate and achieving the same signal-to-noise ratio in a shorter exposure time.

Tracer particles with a density similar to that of target particles but different X-ray attenuation are also attractive approaches. Khan et al. (2011) used potassium iodide as a tracer particle to study the axial motion of glass beads in a rotating drum mixer. As the tracer particles had higher X-ray absorbance than the glass beads, their X-ray radiography results allowed the determination of the tendencies for segregation between the tracer particles and glass beads.

4.2 X-ray stereography

X-ray stereography couples independent 2D X-ray radiographic projections from multiple source-detector pairs to determine the 3D temporal positions of tracer particles. The coupled images track the trajectories and velocity distributions of individual particles in the system of interest. Typically, a frame rate of at least 1000 frames per second (fps) is required to generate phase-distribution images with a spatial resolution of approximately 1 mm. To construct 3D images, projections of the object of interest are acquired simultaneously and consecutively to determine the object's changing position over time. This can be achieved by using multiple source-detector pairs or, if only one source-detector pair is used, by translating or rotating the object to obtain the second projection, as schematically shown in Fig. 7. When the mechanical rotating objects are used, the time resolution of imaging is reduced.

X-ray Particle Tracking Velocimetry (XPTV) includes X-ray stereography and particle tracking techniques to follow the 3D tracer particles' trajectories and velocity over a

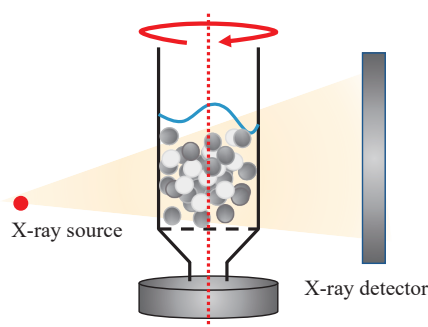


Fig. 7 Schematically drawing of the operating principle of obtaining 2D X-ray projections by rotating the object (fluidized bed).

period of time within the system of interest. XPTV requires the development of robust post-processing algorithms to reduce potential errors caused by factors such as beam hardening and penumbra effects. XPTV provides a balance between spatial and temporal resolutions and has already achieved time resolutions of up to 1000 fps in 2D studies and up to 25 fps in 3D studies 20 years ago (Seeger et al., 2003). Govender et al. (2004) utilized bi-planar X-ray angiography to obtain 3D particle trajectory data in a tumbling mill with a spatial resolution within 0.15 mm, which was used to validate the DEM simulation results. Kingston et al. (2014) developed a so-called cone-beam compensated back-projection algorithm. The geometry of the X-ray beam, which spreads out in a cone shape from the source, was usually assumed to be parallel in XPTV studies. The cone-beam compensated back-projection algorithm corrects for the errors caused by the parallel beam assumption, ensuring that the reconstructed positions and velocities of particles are accurate according to the cone beam assumption.

4.3 X-ray CT

X-ray computed tomography (CT) is an advanced version of X-ray stereography that reconstructs cross-sectional slices by capturing multiple 2D projections of the object. The application of X-ray CT-based techniques in particle motion investigations is also limited by the speed of image acquisition and the trade-off between spatial and temporal resolution. One way to increase the frame rate for rapid X-ray CT is to utilize multiple source-detector pairs, which generate CT slices at rates ranging from 100 Hz to 10 kHz (Saayman, 2013). However, due to the smaller number of projection images from X-ray CT, the spatial resolution is usually limited. X-ray micro-computed tomography systems (micro-CT or μ CT) improve the spatial resolution by controlling the focal spot size and achieve spatial resolutions on the order of a few micrometers. X-ray microscopy (XRM) is a new generation μ CT, which uses optical lenses to magnify the regions of interest within larger samples and achieve resolutions down to 0.5 μ m (Zhu et al., 2022). Even higher resolutions have been achieved by nanofocus

systems (nanoCT, submicronCT) (Kampschulte et al., 2016) or synchrotron-based SR- μ CT (Li et al., 2021), which can achieve spatial resolutions up to 400 nm.

If particles move quickly and the position acquisition rate should be higher than the X-ray CT scanning rate, the particle trajectories (and velocity distribution) will be difficult to determine. Electron beam X-ray CT with a moving electron beam can achieve faster frame rates than traditional X-ray CT with rotating objects or source-detector pairs. Fischer et al. (2008, 2010) reported that ultra-fast electron beam X-ray tomography (UFXCT) can improve image frames from approximately 20 fps (Boyd and Lipton, 1983) to up to 8,000 fps by using linearly scanned electron beams. To track moving systems, Windisch et al. (2020) proposed a control method for UFXCT scanners that self-adjusts the UFXCT scanner based on concurrently acquired images to locate moving structures. The proposed method tracks motion structures within a larger axial range in multiphase flows while simultaneously imaging the environment.

4.4 Recent applications

X-ray radiography and X-ray CT have been widely employed to study particle motion in fluidized beds. X-ray imaging techniques are helpful in understanding and analyzing the complex fluid dynamics and particle motion within fluidized beds, especially for studying void distribution, bubble behavior, jet characteristics, and macroscopic structures within fluidized beds. Errigo et al. (2023a) reviewed and provided insights into the use of X-ray imaging for studying fluidized beds.

Errigo et al. (2023b) used X-ray radiography and infrared thermography to investigate the motion and thermal behavior of large particles (lumps) in high-temperature fluidized beds. They found that the lump density did not have a significant effect on the dispersion coefficient. The optimal fluidization velocities for preventing lump segregation and ensuring proper mixing were identified. These velocity values varied significantly depending on the lump density and bed particle size. Iannello et al. (2022) fabricated core-shell tracer particles consisting of a small lead core and a beech wood or polypropylene outer shell for X-ray imaging analysis. The core-shell tracer particles were injected into a high-temperature fluidized bed reactor. Biomass axial segregation behavior and its interactions with the fluidized bed during the pyrolysis and oxidation stages were studied. The results revealed that the devolatilization behavior of these two materials was largely influenced by the fluidizing medium and independent of the presence of oxygen in the fluidizing medium. The oxidative properties of the fluidized medium did not significantly affect the bubble characteristics or the movement of biomass particles within the fluidized bed. A one-dimensional model was proposed for predicting the axial positions of

particles over time. However, this one-dimensional particle axial position model failed to describe plastic behavior, possibly because of different mechanisms of thermal decomposition reactions.

Bieberle and Barthel (2016) used an ultra-fast X-ray CT system to investigate high particle velocity in a spouted bed. This system allows simultaneous measurements of the velocities of multiple bed particles, achieving speeds of up to 8000 fps with a spatial resolution of 1 mm. Waktola et al. (2018) used ROFEX (Rossendorf fast electron beam X-ray tomography) with a novel image processing method to study the gravitational flow of granular materials in various types of silos. Their approach was capable of obtaining the velocity, lateral movement, and three-dimensional rotation of individual particles. Stannarius et al. (2019) employed ultra-fast X-ray computed tomography to observe the discharging of hard, frictional grain spheres and soft, low-friction hydrogel spheres in cylindrical containers through small orifices. An imaging speed of 1000 fps was shown to provide sufficient temporal resolution for identifying individual particles passing through the orifices. The analysis of the collected time-resolved images also enabled the characterization of the fundamentals of the internal flow field. The results indicate that the flow-field structures during silo discharge differ inherently between these two types of particles.

Non-spherical particles exhibit anisotropy, where their resistance varies with orientation, resulting in motion and trajectories that are considerably different from those of spherical particles. X-ray imaging techniques have been used to study the motion of non-spherical particles. Non-spherical particles tend to have different mixing-segregation and fluidization behaviors from spherical particles. Chen et al. (2019a, 2019b) employed cylindrical particles as representative non-spherical particles co-fluidized with spherical particles in a binary fluidized bed, and investigated the dynamics using XPTV. The effects of sphericity, size, particle mass fraction, and superficial gas velocity on the position, velocity, and 3D orientation of cylindrical tracer particles were reported. Increasing the superficial gas velocity slightly improved the uniformity of both the vertical and horizontal distributions of cylindrical particles. Cylindrical particles were found to be more prevalent in the near-wall region than in the center region of the bed. A model was proposed to describe the orientation distribution of cylindrical particles. Yang and Fu (2004) used Celphre™ impregnated with lead (II) acetate as the tracer particles to study compaction and mixing characteristics in a V-blender. They reported significant particle rearrangement during the initial stages of mold compaction. The effects of particle size and initial loading configuration on mixing efficiency in the V-blender were also investigated.

X-ray CT for process analysis usually requires interrupting the measurement process, making it unsuitable for

real-time online monitoring tools. By inserting a 304 stainless steel wire into the particle of interest, Nadeem et al. (2023a) labeled a single particle for tracking. They employed the concept of ergodicity and tracked a single tracer particle over a sufficiently long period using 60-fps X-ray radiography with two X-ray sources positioned 90° apart. Three different traditional mixing indices, standard deviation-based Location Distribution Mixing Index (LDMI), Modified Generalized Mixing Mean Mixing Index (MGMMI), and Gini Index, were used to quantify the degree of mixing. LDMI is calculated based on the standard deviation of the tracer concentration in the samples at some specific time; MGMMI is the location-based mixing index calculated according to temporal observations of the tracer particle's concentration at a specific location; and Gini Index is based on statistical dispersion calculated utilizing the Lorenz curve. The details are given in Nadeem et al. (2023a). It was found that the LDMI index is suitable for determining mixing homogeneity values, whereas the Gini index is suitable for predicting mixing endpoints. The proposed method, which is similar to the PEPT algorithm, offers faster imaging and data acquisition speeds, enabling real-time degree of mixture monitoring. Nadeem et al. (2023c) used X-ray CT to study the mixing of a vertical blade mixer. The researchers captured CT images at different mixing stages and extracted detailed particle distributions of binary mixtures composed of particles with different densities within the mixing vessel. A new mixing index, generalized nearest neighbor (GNN), was defined to quantify the degree of mixing. They used X-ray CT and GNN indices to evaluate the effects of density and size of particles, filling ratio, and blade rotational speed on the evolution of mixing (Nadeem et al., 2023b). The GNN mixing index was compared to other mixing indices, including those based on standard deviation and position. The GNN mixing index can reliably quantify mixture homogeneity at the particle scale. Ho et al. (2023) used 3D X-ray μ CT analysis to evaluate the mixing performance of two different particle sizes and densities in a lab-scale agitator filter dryer. Their work employed AI-based image analytics to derive mixing indices and mixing kinetics. They observed that after several cycles of mixing, axial and radial interpenetration occurred, resulting in a progressively uniform distribution.

5. Magnetic Resonance Imaging (MRI)

Magnetic Resonance Imaging is a technique that uses the principles of nuclear magnetic resonance for imaging. Nuclei with nuclear spins have uneven numbers of protons and neutrons, such as ^1H , ^{13}C , ^{19}F , ^{23}Na , ^{31}P , ^{129}Xe . ^1H is particularly abundant in biological tissues, making it the most commonly used isotope in medical MRI. The MRI principles are schematically illustrated in Fig. 8. When conducting MRI, an external magnetic field B_0 is applied to

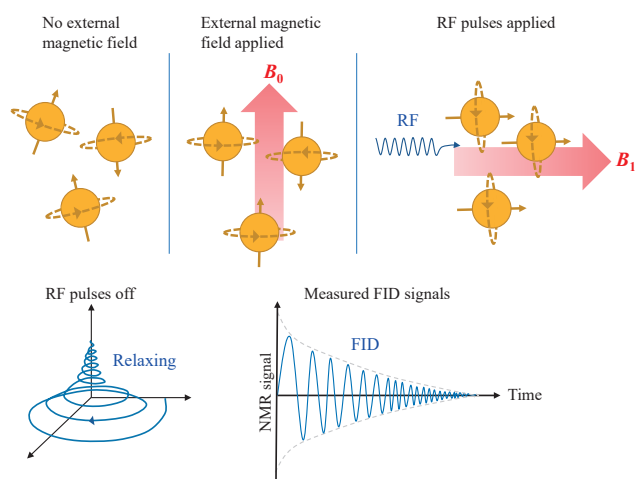


Fig. 8 Schematic diagrams illustrating the principles of MRI.

a system of interest, which aligns the spin-induced magnetization of the atomic nuclei with net nuclear spin in a direction parallel to B_0 . One or a series of radio frequency (RF) pulses is then applied to the system to excite the B_0 -aligned nuclei, such that their magnetization vector changes from parallel to perpendicular to B_0 , creating perpendicular magnetic field B_1 . After the RF pulse, the excited nuclei gradually relax to their original parallel magnetization orientation. If the system of interest is heterogeneous, i.e., containing distinct domains with different properties, the nuclei in its different domains will relax at different speeds. Therefore, the relaxation speed of a nucleus provides information about its domain identity. The relaxation speeds of all excited nuclei are extracted from the recorded change of the nuclei's magnetization orientations, termed Free Induction Decay (FID), from which domains within the system can be identified.

Spatial information about the domains, including location, size, shape, and other factors, is determined by making B_0 a gradient field and varying the bandwidth of the RF pulses for excitation. The captured images can be 1D images averaged over cross-sections, vertical 2D slices, horizontal 2D slices, or 3D images. In MRI technology, the relaxation time of liquids is typically much longer than that of solids, making them more detectable by the receiver coils of MRI. Therefore, liquid-containing particles are a primary choice as tracer particles in MRI particle motion studies. Various liquid-containing natural and artificial particles have been used as tracers, including oil-rich seeds (such as mustard and poppy seeds) and porous particles saturated with liquid. For systems whose particles lack MRI-active nuclei, tracer particles containing abundant MRI-active nuclei can be added (either directly or incorporated into the tracer particle) to aid particle motion tracking. For particle motion investigation systems, particles can be imaged positively or negatively. NMR signal intensity usually requires the use of calibration techniques to

convert NMR signals to concentration maps for imaging.

The advantage of MRI as a tool for understanding particle motions is its safety, as it does not involve high-energy radiation. MRI also provides reasonable spatial resolution, the ability to discern different materials, and the ability to measure the velocity distributions of particles using “tagging methods” or “phase methods”. The drawbacks of this approach include the lower imaging speeds, which affect temporal resolution, magnetic interference from metal components, and lower material selectivity compared with X-ray CT. Practical MRI typically handles particle systems that are smaller than several tens of centimeters in dimensions, making larger particle system analyses unsuitable for MRI. To address the issue of slow imaging speed, rapid MRI techniques, such as Echo Planar Imaging (EPI), Rapid Acquisition with Relaxation Enhancement (RARE), and fast low angle shooting (FLASH), have been developed. The state-of-the-art ultra-short echo time magnetic resonance imaging (UTE MRI) achieves spatial and temporal resolutions of 1 mm and 25 ms for 2D slice images, respectively (Fabich et al., 2017). The UTE MRI technique may be sufficient to determine macroscopic fluid dynamics in most unsteady particle-fast-moving fluidized bed systems.

5.1 Recent applications

MRI technologies have been used to study particle mixing and separation in mixers. They provide a clear visualization of front evolution in binary mixing systems and distinguish the effects of particle size and density ratios on radial and axial segregation (Hill et al., 1997; Nakagawa, 1994; Nguyễn et al., 2011; Rao et al., 1991). Mihailova et al. (2015) combined PEPT and MRI techniques to study the mixing, local velocity, and concentration fields of two streams of Newtonian fluid glycerol in a laminar flow static mixer. These two glycerol streams contained different concentrations of $GdCl_3$ NMR contrast agent. This work demonstrated the potential to study particle behavior using PEPT and fluid behavior using MRI in solid–liquid two-phase systems, providing a comprehensive characterization of particle motion processes. Penn et al. (2017) used medical MRI to study particle dynamics. They designed and manufactured spherical, non-cohesive core-shell particles with customized mechanical and NMR properties. These engineered particles exhibited higher signal strength and longer lifetimes than normal agricultural seeds. The real-time data acquisition speed was increased by four orders of magnitude using various scan acceleration techniques. The same team later conducted several studies using this real-time MRI for gas–solid fluidized beds. The particle concentrations and motion under different bubbling conditions with temporal resolutions of 7 and 18 ms were visualized (Penn et al., 2018). The same team also examined the influence of the internal components on the fluidization dynamics (Penn et al., 2019). The impact of liquid bridging

Table 4 Comparison of four radiation-based investigation techniques for understanding particle motion.

	RPT	PEPT	X-ray-based method	MRI
Pros	<ul style="list-style-type: none"> • High sensitivity • Versatility • Relatively simple data processing 	<ul style="list-style-type: none"> • High temporal and spatial resolution 	<ul style="list-style-type: none"> • High accessibility 	<ul style="list-style-type: none"> • High spatial resolution • No radioactivity
Cons	<ul style="list-style-type: none"> • Comprehensive calibration is required • Longer measurement time 	<ul style="list-style-type: none"> • Expensive • Short lifespans of positron emitters • Limited number of tracked particles 	<ul style="list-style-type: none"> • Specific data processing is required. • Limited to 2D imaging 	<ul style="list-style-type: none"> • More imaging time is required. • Limited selection of tracers • Restrictions on metals

between particles in the gas–solid fluidized bed on hydrodynamics was investigated by MRI (Boyce et al., 2018).

Advances in MRI hardware, reconstruction methods, and experimental design have led to notable progress in applying MRI technologies to studying particle motions. Several reviews have extensively chronicled these MRI technique advancements (Bonn et al., 2008; Clarke et al., 2025; Fukushima, 1999; Kawaguchi, 2010; Stannarius, 2017). The MRI data were used to validate the simulation predictions. Xi et al. used MRI studies on particle and bubble dynamics (Penn et al., 2018) to examine the accuracy of TFM (Xi et al., 2021a) and CFD-DEM (Xi et al., 2021b) simulations. They found that these simulation models could predict the relationship between the bubble diameter and bubble count with bed height, but they underestimated the particle velocities.

6. Conclusion

The principles, advances, and recent applications of RPT, PEPT, X-ray-based methods, and MRI techniques in studying particle motion in processes are reviewed. These techniques are generally non-invasive, have a large signal-penetration distance, and offer high sensitivity; however, they are generally costly and require extensive safety precautions. A comparison of these techniques based on their advantages and disadvantages is summarized in Table 4. MRI offers a safer alternative but is generally limited in terms of the size of the interrogation volume. X-ray-based methods provide macroscopic visualization of particle motion, whereas RPT, PEPT, and MRI offer insights into the dynamics of individual particles at the microscopic level. Between the γ -ray-powered RPT and PEPT, RPT is better suited to large-volume systems than PEPT because of its lower cost and versatility, whereas the PEPT offers better resolution. Each of the four reviewed techniques has its strengths and weaknesses, and selection among them should be based on a comprehensive consideration of specific experimental purposes, application scenarios, and other requirements. Significant advancements in both hardware and software for these techniques have contributed to enhancements in imaging and tracking accuracy in the past few decades. Recently, use of artificial intelligence

and other computer-aided data extraction methods has brought further improvements.

References

- Al-Juwaya T., Ali N., Al-Dahhan M., Experimental validation of the mechanistic scale-up methodology of gas–solid spouted beds using radioactive particle tracking (RPT), *Annals of Nuclear Energy*, 181 (2023) 109559. <https://doi.org/10.1016/j.anucene.2022.109559>
- Al-Shemmeri M., Windows-Yule K., Lopez-Quiroga E., Fryer P.J., Coffee bean particle motion in a spouted bed measured using positron emission particle tracking (PEPT), *Journal of Food Engineering*, 311 (2021) 110709. <https://doi.org/10.1016/j.jfoodeng.2021.110709>
- Al-Shemmeri M., Windows-Yule K., Lopez-Quiroga E., Fryer P.J., Coffee bean particle motion in a rotating drum measured using Positron Emission Particle Tracking (PEPT), *Food Research International*, 163 (2023) 112253. <https://doi.org/10.1016/j.foodres.2022.112253>
- Ali N., Al-Juwaya T., Al-Dahhan M., An advanced evaluation of spouted beds scale-up for coating TRISO nuclear fuel particles using radioactive particle tracking (RPT), *Experimental Thermal and Fluid Science*, 80 (2017a) 90–104. <https://doi.org/10.1016/j.expthermflusci.2016.08.002>
- Ali N., Al-Juwaya T., Al-Dahhan M., An advanced evaluation of the mechanistic scale-up methodology of gas–solid spouted beds using radioactive particle tracking, *Particuology*, 34 (2017b) 48–60. <https://doi.org/10.1016/j.partic.2016.11.005>
- Bhusarapu S., Al-Dahhan M.H., Duduković M.P., Trujillo S., O'Hern T.J., Experimental study of the solids velocity field in gas–solid risers, *Industrial & Engineering Chemistry Research*, 44 (2005) 9739–9749. <https://doi.org/10.1021/ie050297f>
- Bieberle M., Barthel F., Combined phase distribution and particle velocity measurement in spout fluidized beds by ultrafast X-ray computed tomography, *Chemical Engineering Journal*, 285 (2016) 218–227. <https://doi.org/10.1016/j.cej.2015.10.003>
- Biswal J., Goswami S., Upadhyay R.K., Pant H.J., Methods of preparation of microparticles for radioactive particle tracking experiments, *Applied Radiation and Isotopes*, 168 (2021) 109380. <https://doi.org/10.1016/j.apradiso.2020.109380>
- Bonn D., Rodts S., Groeninck M., Rafai S., Shahidzadeh-Bonn N., Coussot P., Some applications of magnetic resonance imaging in fluid mechanics: complex flows and complex fluids, *Annual Review of Fluid Mechanics*, 40 (2008) 209–233. <https://doi.org/10.1146/annurev.fluid.40.111406.102211>
- Boucher D., Deng Z., Leadbeater T., Langlois R., Waters K.E., Observation of iron ore beneficiation within a spiral concentrator by positron emission particle tracking of large ($\phi = 1440 \mu\text{m}$) and small ($\phi = 58 \mu\text{m}$) hematite and quartz tracers, *Chemical Engineering Science*, 140 (2016) 217–232. <https://doi.org/10.1016/j.ces.2015.10.018>
- Boyce C.M., Penn A., Pruessmann K.P., Müller C.R., Magnetic resonance imaging of gas–solid fluidization with liquid bridging, *AIChE Journal*, 64 (2018) 2958–2971. <https://doi.org/10.1002/aic.16036>
- Boyd D.P., Lipton M.J., Cardiac computed tomography, *Proceedings of the IEEE*, 71 (1983) 298–307.

- <https://doi.org/10.1109/PROC.1983.12588>
- Broadbent C., Bridgwater J., Parker D., Keningley S., Knight P., A phenomenological study of a batch mixer using a positron camera, *Powder Technology*, 76 (1993) 317–329.
[https://doi.org/10.1016/S0032-5910\(05\)80013-0](https://doi.org/10.1016/S0032-5910(05)80013-0)
- Burnard D., Caden A., Gargiuli J., Leadbeater T., Parker D., Griffiths W.D., A positron emission particle tracking (PEPT) study of inclusions in liquid aluminium alloy, *Advanced Materials Research*, 922 (2014) 43–48.
<https://doi.org/10.4028/www.scientific.net/AMR.922.43>
- Che H., Al-Shemmeri M., Fryer P.J., Lopez-Quiroga E., Wheldon T.K., Windows-Yule K., PEPT validated CFD-DEM model of aspherical particle motion in a spouted bed, *Chemical Engineering Journal*, 453 (2023a) 139689. <https://doi.org/10.1016/j.cej.2022.139689>
- Che H., Werner D., Seville J., Wheldon T.K., Windows-Yule K., Evaluation of coarse-grained CFD-DEM models with the validation of PEPT measurements, *Particuology*, 82 (2023b) 48–63.
<https://doi.org/10.1016/j.partic.2022.12.018>
- Chen X., Zhong W., Heindel T.J., Orientation of cylindrical particles in a fluidized bed based on stereo X-ray particle tracking velocimetry (XPTV), *Chemical Engineering Science*, 203 (2019a) 104–112.
<https://doi.org/10.1016/j.ces.2019.03.067>
- Chen X., Zhong W., Heindel T.J., Using stereo XPTV to determine cylindrical particle distribution and velocity in a binary fluidized bed, *AIChE Journal*, 65 (2019b) 520–535.
<https://doi.org/10.1002/aic.16485>
- Clarke D.A., Hogendoorn W., Penn A., Serial M.R., Magnetic resonance imaging in granular flows: an overview of recent advances, *Particuology*, 101 (2025) 18–32.
<https://doi.org/10.1016/j.partic.2023.08.007>
- Cole K., Barker D.J., Brito-Parada P.R., Buffler A., Hadler K., Mackay I., Mesa D., Morrison A.J., Neethling S., Norori-McCormac A., Standard method for performing positron emission particle tracking (PEPT) measurements of froth flotation at PEPT Cape Town, *MethodsX*, 9 (2022a) 101680.
<https://doi.org/10.1016/j.mex.2022.101680>
- Cole K., Brito-Parada P.R., Hadler K., Mesa D., Neethling S.J., Norori-McCormac A.M., Cilliers J.J., Characterisation of solid hydrodynamics in a three-phase stirred tank reactor with positron emission particle tracking (PEPT), *Chemical Engineering Journal*, 433 (2022b) 133819. <https://doi.org/10.1016/j.cej.2021.133819>
- Cole K., Buffler A., Cilliers J., Govender I., Heng J., Liu C., Parker D., Shah U., van Heerden M., Fan X., A surface coating method to modify tracers for positron emission particle tracking (PEPT) measurements of froth flotation, *Powder Technology*, 263 (2014) 26–30.
<https://doi.org/10.1016/j.powtec.2014.04.083>
- de Freitas Dam R.S., Affonso R.R.W., Salgado W.L., Schirru R., Salgado C.M., A comparative study of a traditional localization algorithm and a deep learning model for radioactive particle tracking application, *Applied Radiation and Isotopes*, 205 (2024) 111156.
<https://doi.org/10.1016/j.apradiso.2023.111156>
- de Freitas Dam R.S., dos Santos M.C., do Desterro F.S.M., Salgado W.L., Schirru R., Salgado C.M., A novel radioactive particle tracking algorithm based on deep rectifier neural network, *Nuclear Engineering and Technology*, 53 (2021) 2334–2340.
<https://doi.org/10.1016/j.net.2021.01.002>
- de Freitas Dam R.S., Teixeira T.P., Salgado W.L., Salgado C.M., A new application of radioactive particle tracking using MCNPX code and artificial neural network, *Applied Radiation and Isotopes*, 149 (2019) 38–47. <https://doi.org/10.1016/j.apradiso.2019.04.011>
- Devanathan N., Moslemian D., Dudukovic M., Flow mapping in bubble columns using CARPT, *Chemical Engineering Science*, 45 (1990) 2285–2291. [https://doi.org/10.1016/0009-2509\(90\)80107-P](https://doi.org/10.1016/0009-2509(90)80107-P)
- Doucet J., Bertrand F., Chaouki J., An extended radioactive particle tracking method for systems with irregular moving boundaries, *Powder Technology*, 181 (2008) 195–204.
<https://doi.org/10.1016/j.powtec.2006.12.019>
- Dubé O., Dubé D., Chaouki J., Bertrand F., Optimization of detector positioning in the radioactive particle tracking technique, *Applied Radiation and Isotopes*, 89 (2014) 109–124.
<https://doi.org/10.1016/j.apradiso.2014.02.019>
- Efhaima A., Al-Dahhan M.H., Assessment of scale-up dimensionless groups methodology of gas-solid fluidized beds using advanced non-invasive measurement techniques (CT and RPT), *The Canadian Journal of Chemical Engineering*, 95 (2017) 656–669.
<https://doi.org/10.1002/cjce.22745>
- Errigo M., Lettieri P., Materazzi M., X-ray imaging techniques for gas-solid fluidized beds: a technical review, *Particuology*, (2023a).
<https://doi.org/10.1016/j.partic.2023.11.013>
- Errigo M., Sebastiani A., Iannello S., Materazzi M., Lettieri P., Application of imaging techniques for the characterization of lumps behaviour in gas-solid fluidized-bed reactors, *Fuel*, 349 (2023b) 128634. <https://doi.org/10.1016/j.fuel.2023.128634>
- Fabich H.T., Sederman A.J., Holland D.J., Study of bubble dynamics in gas-solid fluidized beds using ultrashort echo time (UTE) magnetic resonance imaging (MRI), *Chemical Engineering Science*, 172 (2017) 476–486. <https://doi.org/10.1016/j.ces.2017.07.003>
- Fan X., Parker D., Smith M., Labelling a single particle for positron emission particle tracking using direct activation and ion-exchange techniques, *Nuclear Instruments and Methods in Physics Research Section A: Accelerators, Spectrometers, Detectors and Associated Equipment*, 562 (2006) 345–350.
<https://doi.org/10.1016/j.nima.2006.03.015>
- Fangary Y., Barigou M., Seville J., Parker D., Fluid trajectories in a stirred vessel of non-newtonian liquid using positron emission particle tracking, *Chemical Engineering Science*, 55 (2000) 5969–5979.
[https://doi.org/10.1016/S0009-2509\(00\)00176-7](https://doi.org/10.1016/S0009-2509(00)00176-7)
- Fischer F., Hampel U., Ultra fast electron beam X-ray computed tomography for two-phase flow measurement, *Nuclear Engineering and Design*, 240 (2010) 2254–2259.
<https://doi.org/10.1016/j.nucengdes.2009.11.016>
- Fischer F., Hoppe D., Schleicher E., Mattausch G., Flaske H., Bartel R., Hampel U., An ultra fast electron beam X-ray tomography scanner, *Measurement Science and Technology*, 19 (2008) 094002.
<https://doi.org/10.1088/0957-0233/19/9/094002>
- Forster R., Seville J., Parker D., Ding Y., Tracking single particles in process equipment or probing processes using positrons, *KONA Powder and Particle Journal*, 18 (2000) 139–148.
<https://doi.org/10.14356/kona.2000020>
- Fukushima E., Nuclear magnetic resonance as a tool to study flow, *Annual Review of Fluid Mechanics*, 31 (1999) 95–123.
<https://doi.org/10.1146/annurev.fluid.31.1.95>
- Godfroy L., Larachi F., Kennedy G., Grandjean B., Chaouki J., On-line flow visualization in multiphase reactors using neural networks, *Applied Radiation and Isotopes*, 48 (1997) 225–235.
[https://doi.org/10.1016/S0969-8043\(96\)00183-2](https://doi.org/10.1016/S0969-8043(96)00183-2)
- González S., Windows-Yule C., Luding S., Parker D., Thornton A.R., Forced axial segregation in axially inhomogeneous rotating systems, *Physical Review E*, 92 (2015) 022202.
<https://doi.org/10.1103/PhysRevE.92.022202>
- Govender I., Cleary P., Mainza A., Comparisons of PEPT derived charge features in wet milling environments with a friction-adjusted DEM model, *Chemical Engineering Science*, 97 (2013) 162–175.
<https://doi.org/10.1016/j.ces.2013.04.023>
- Govender I., McBride A., Powell M., Improved experimental tracking techniques for validating discrete element method simulations of tumbling mills, *Experimental Mechanics*, 44 (2004) 593–607.
- Guida A., Fan X., Parker D., Nienow A., Barigou M., Positron emission particle tracking in a mechanically agitated solid-liquid suspension of coarse particles, *Chemical Engineering Research and Design*, 87 (2009) 421–429. <https://doi.org/10.1016/j.cherd.2008.12.001>
- Guida A., Nienow A.W., Barigou M., PEPT measurements of solid-liquid flow field and spatial phase distribution in concentrated mono-disperse stirred suspensions, *Chemical Engineering Science*, 65 (2010) 1905–1914. <https://doi.org/10.1016/j.ces.2009.11.005>
- Hart-Villamil R., Ingram A., Windows-Yule C., Gupta S., Nicușan A.L., On the autonomous validation and comparison of particle models for a Newtonian laminar flow mixing model using PEPT, *Chemical Engineering Research and Design*, 206 (2024) 139–150.
<https://doi.org/10.1016/j.cherd.2024.04.023>

- Hawkesworth M., O'Dwyer M., Walker J., Fowles P., Heritage J., Stewart P., Witcomb R., Bateman J., Connolly J., Stephenson R., A positron camera for industrial application, *Nuclear Instruments and Methods in Physics Research Section A: Accelerators, Spectrometers, Detectors and Associated Equipment*, 253 (1986) 145–157. [https://doi.org/10.1016/0168-9002\(86\)91138-1](https://doi.org/10.1016/0168-9002(86)91138-1)
- He Y.-L., Lim C., Grace J., Scale-up studies of spouted beds, *Chemical Engineering Science*, 52 (1997) 329–339. [https://doi.org/10.1016/S0009-2509\(96\)00378-8](https://doi.org/10.1016/S0009-2509(96)00378-8)
- Herald M., Bingham Z., Santos R., Ruggles A., Simulated time-dependent data to estimate uncertainty in fluid flow measurements, *Nuclear Engineering and Design*, 337 (2018) 221–227. <https://doi.org/10.1016/j.nucengdes.2018.07.005>
- Herald M., Wheldon T., Windows-Yule C., Monte Carlo model validation of a detector system used for positron emission particle tracking, *Nuclear Instruments and Methods in Physics Research Section A: Accelerators, Spectrometers, Detectors and Associated Equipment*, 993 (2021) 165073. <https://doi.org/10.1016/j.nima.2021.165073>
- Hill K.M., Caprihan A., Kakalios J., Bulk segregation in rotated granular material measured by magnetic resonance imaging, *Physical Review Letters*, 78 (1997) 50. <https://doi.org/10.1103/PhysRevLett.78.50>
- Ho R., Shin Y., Zhang S., Zhu A., Kumar P., Goyal H., Advanced image analytics to study powder mixing in a novel laboratory scale agitated filter dryer, *Powder Technology*, 417 (2023) 118273. <https://doi.org/10.1016/j.powtec.2023.118273>
- Huang A.N., Cheng T.H., Hsu W.Y., Huang C.C., Kuo H.P., DEM study of particle segregation in a rotating drum with internal diameter variations, *Powder Technology*, 378 (2021a) 430–440. <https://doi.org/10.1016/j.powtec.2020.10.019>
- Huang A.N., Liu L.C., Kuo H.P., The role of end wall shearing in the drum segregation band formation, *Powder Technology*, 239 (2013) 98–104. <https://doi.org/10.1016/j.powtec.2013.01.042>
- Huang A.N., Wang X., Hsu W.Y., Kuo H.P., Particle segregation in a rotating drum with inner segmentation ring pair, *Powder Technology*, 394 (2021b) 891–900. <https://doi.org/10.1016/j.powtec.2021.09.015>
- Iannello S., Foscolo P.U., Materazzi M., Investigation of single particle devolatilization in fluidized bed reactors by X-ray imaging techniques, *Chemical Engineering Journal*, 431 (2022) 133807. <https://doi.org/10.1016/j.cej.2021.133807>
- Ingram A., Hausard M., Fan X., Parker D., Seville J., Finn N., Evans M., Portable positron emission particle tracking (PEPT) for industrial use, in “The 12th International Conference on Fluidization—New Horizons in Fluidization Engineering”, (2007). https://dc.engconfintl.org/fluidization_xii/60
- Jayasundara C.T., Yang R., Guo B., Yu A., Govender I., Mainza A., van der Westhuizen A., Rubenstein J., CFD–DEM modelling of particle flow in IsaMills—Comparison between simulations and PEPT measurements, *Minerals Engineering*, 24 (2011) 181–187. <https://doi.org/10.1016/j.mineng.2010.07.011>
- Jones-Salkey O., Nicusan A., Windows-Yule C., Ingram A., Werner D., Clifford S., Reynolds G., Application of positron emission particle tracking (PEPT) for the evaluation of powder behaviour in an incline linear blender for continuous direct compression (CDC), *International Journal of Pharmaceutics*, 645 (2023) 123361. <https://doi.org/10.1016/j.ijpharm.2023.123361>
- Kalo L., Pant H.J., Upadhyay R.K., Validation of the glicksman scaling law for gas–solid conical fluidized beds using the radioactive particle tracking technique, *Industrial & Engineering Chemistry Research*, 59 (2020) 20943–20952. <https://doi.org/10.1021/acs.iecr.0c03287>
- Kamalanathan P., Kalo L., Pant H.J., Upadhyay R.K., Effect of dynamic bias on accuracy of radioactive particle tracking (RPT) technique at different data acquisition frequencies, *Applied Radiation and Isotopes*, 128 (2017) 13–21. <https://doi.org/10.1016/j.apradiso.2017.06.034>
- Kampschulte M., Langheinrich A., Sender J., Litzlbauer H., Althöhn U., Schwab J., Alexandre-Lafont E., Martels G., Krombach G., Nano-computed tomography: technique and applications, *Fortschr Röntgenstr*, 188 (2016) 146–154. <https://doi.org/10.1055/s-0041-106541>
- Kawaguchi T., MRI measurement of granular flows and fluid-particle flows, *Advanced Powder Technology*, 21 (2010) 235–241. <https://doi.org/10.1016/j.appt.2010.03.014>
- Khan Z., Van Bussel F., Schaber M., Seemann R., Scheel M., Di Michiel M., High-speed measurement of axial grain transport in a rotating drum, *New Journal of Physics*, 13 (2011) 105005. <https://doi.org/10.1088/1367-2630/13/10/105005>
- Kingston T.A., Geick T.A., Robinson T.R., Heindel T.J., Characterizing 3D granular flow structures in a double screw mixer using X-ray particle tracking velocimetry, *Powder Technology*, 278 (2015) 211–222. <https://doi.org/10.1016/j.powtec.2015.02.061>
- Kingston T.A., Morgan T.B., Geick T.A., Robinson T.R., Heindel T.J., A cone-beam compensated back-projection algorithm for X-ray particle tracking velocimetry, *Flow Measurement and Instrumentation*, 39 (2014) 64–75. <https://doi.org/10.1016/j.flowmeasinst.2014.06.002>
- Kondukov N., Kornilaev A., Skachko I., Akhromenkov A., Kruglov A., An investigation of the parameters of moving particles in a fluidized bed by a radioisotopic method, *International Chemical Engineering*, 4 (1964) 43.
- Kuo H.P., Knight P., Parker D., Adams M., Seville J., Discrete element simulations of a high-shear mixer, *Advanced Powder Technology*, 15 (2004) 297–309. <https://doi.org/10.1163/156855204774150109>
- Kuo H.P., Knight P., Parker D., Burbidge A., Adams M., Seville J., Non-equilibrium particle motion in the vicinity of a single blade, *Powder Technology*, 132 (2003) 1–9. [https://doi.org/10.1016/S0032-5910\(02\)00316-9](https://doi.org/10.1016/S0032-5910(02)00316-9)
- Kuo H.P., Knight P., Parker D., Seville J., Solids circulation and axial dispersion of cohesionless particles in a V-mixer, *Powder Technology*, 152 (2005) 133–140. <https://doi.org/10.1016/j.powtec.2004.12.003>
- Kuo H.P., Knight P., Parker D., Tsuji Y., Adams M., Seville J., The influence of DEM simulation parameters on the particle behaviour in a V-mixer, *Chemical Engineering Science*, 57 (2002) 3621–3638. [https://doi.org/10.1016/S0009-2509\(02\)00086-6](https://doi.org/10.1016/S0009-2509(02)00086-6)
- Kuo H.P., Tseng W.T., Huang A.N., Controlling of segregation in rotating drums by independent end wall rotations, *KONA Powder and Particle Journal*, 33 (2016) 239–248. <https://doi.org/10.14356/kona.2016004>
- Langford S., Wiggins C., Tenpenny D., Ruggles A., Positron emission particle tracking (PEPT) for fluid flow measurements, *Nuclear Engineering and Design*, 302 (2016) 81–89. <https://doi.org/10.1016/j.nucengdes.2016.01.017>
- Larachi F., Kennedy G., Chaouki J., A γ -ray detection system for 3-D particle tracking in multiphase reactors, *Nuclear Instruments and Methods in Physics Research Section A: Accelerators, Spectrometers, Detectors and Associated Equipment*, 338 (1994) 568–576. [https://doi.org/10.1016/0168-9002\(94\)91343-9](https://doi.org/10.1016/0168-9002(94)91343-9)
- Laverman J., Fan X., Ingram A., van Sint Annaland M., Parker D., Seville J., Kuipers J., Experimental study on the influence of bed material on the scaling of solids circulation patterns in 3D bubbling gas–solid fluidized beds of glass and polyethylene using positron emission particle tracking, *Powder Technology*, 224 (2012) 297–305. <https://doi.org/10.1016/j.powtec.2012.03.011>
- Leadbeater T., Buffler A., van Heerden M., Camroodien A., Steyn D., Development of tracer particles for positron emission particle tracking, *Nuclear Science and Engineering*, 198 (2024) 121–137. <https://doi.org/10.1080/00295639.2023.2171234>
- Leadbeater T., Parker D., A modular positron camera for the study of industrial processes, *Nuclear Instruments and Methods in Physics Research Section A: Accelerators, Spectrometers, Detectors and Associated Equipment*, 652 (2011) 646–649. <https://doi.org/10.1016/j.nima.2010.08.085>
- Leadbeater T.W., Seville J.P., Parker D.J., On trajectory and velocity measurements in fluidized beds using positron emission particle tracking (PEPT), *The Canadian Journal of Chemical Engineering*, 101 (2023) 269–282. <https://doi.org/10.1002/cjce.24622>
- Lee K.S., Kim T.J., Pratz G., Single-cell tracking with PET using a novel trajectory reconstruction algorithm, *IEEE Transactions on Medical Imaging*, 34 (2014) 994–1003. <https://doi.org/10.1109/TMI.2014.2373351>
- Li C., Zhang Y., Zhu N., Emady H.N., Zhang L., Experimental investiga-

- tion of wet pharmaceutical granulation using in-situ synchrotron X-ray imaging, *Powder Technology*, 378 (2021) 65–75. <https://doi.org/10.1016/j.powtec.2020.09.063>
- Lin C.L., Miller J.D., Cortes A., Applications of X-ray computed tomography in particulate systems, *KONA Powder and Particle Journal*, 10 (1992) 88–95. <https://doi.org/10.14356/kona.1992013>
- Lin J., Chen M., Chao B., A novel radioactive particle tracking facility for measurement of solids motion in gas fluidized beds, *AIChE Journal*, 31 (1985) 465–473. <https://doi.org/10.1002/aic.690310314>
- Lindner G., Shi S., Vučetić S., Mišković S., Transfer learning for radioactive particle tracking, *Chemical Engineering Science*, 248 (2022) 117190. <https://doi.org/10.1016/j.ces.2021.117190>
- Mandel S., Machine learning is used to conduct positron emission particle tracking, *Scilight*, 4 (2020) 041110. <https://doi.org/10.1063/1.5000633>
- Mesa D., van Heerden M., Cole K., Neethling S.J., Brito-Parada P.R., Hydrodynamics in a three-phase flotation system—fluid following with a new hydrogel tracer for positron emission particle tracking (PEPT), *Chemical Engineering Science*, 260 (2022) 117842. <https://doi.org/10.1016/j.ces.2022.117842>
- Mihailova O., Lim V., McCarthy M.J., McCarthy K.L., Bakalis S., Laminar mixing in a SMX static mixer evaluated by positron emission particle tracking (PEPT) and magnetic resonance imaging (MRI), *Chemical Engineering Science*, 137 (2015) 1014–1023. <https://doi.org/10.1016/j.ces.2015.07.015>
- Mittal A., Kumar M., Mangadoddy N., A coupled CFD–DEM model for tumbling mill dynamics—Effect of lifter profile, *Powder Technology*, 433 (2024) 119178. <https://doi.org/10.1016/j.powtec.2023.119178>
- Moodley T.L., Govender I., Experimental validation of DEM in rotating drums using positron emission particle tracking, *Mechanics Research Communications*, 121 (2022) 103861. <https://doi.org/10.1016/j.mechrescom.2022.103861>
- Morrison A., Govender I., Mainza A., Parker D., The shape and behaviour of a granular bed in a rotating drum using Eulerian flow fields obtained from PEPT, *Chemical Engineering Science*, 152 (2016) 186–198. <https://doi.org/10.1016/j.ces.2016.06.022>
- Mosorov V., Abdullah J., MCNP5 code in radioactive particle tracking, *Applied Radiation and Isotopes*, 69 (2011) 1287–1293. <https://doi.org/10.1016/j.apradiso.2011.04.028>
- Nadeem H., Jamdagni P., Subramaniam S., Nere N.K., Heindel T.J., Assessing solid particle mixing using X-ray radiographic particle tracking, *Chemical Engineering Research and Design*, 194 (2023a) 563–572. <https://doi.org/10.1016/j.cherd.2023.05.003>
- Nadeem H., Jamdagni P., Subramaniam S., Nere N.K., Heindel T.J., Non-invasive particle-scale investigation of the effects of blade speed and particle properties on mixture homogeneity evolution using X-ray CT, *Chemical Engineering Science*, 276 (2023b) 118766. <https://doi.org/10.1016/j.ces.2023.118766>
- Nadeem H., Subramaniam S., Nere N.K., Heindel T.J., A particle scale mixing measurement method using a generalized nearest neighbor mixing index, *Advanced Powder Technology*, 34 (2023c) 103933. <https://doi.org/10.1016/j.appt.2022.103933>
- Nakagawa M., Axial segregation of granular flows in a horizontal rotating cylinder, *Chemical Engineering Science*, 49 (1994) 2540–2544. [https://doi.org/10.1016/0009-2509\(94\)E0086-6](https://doi.org/10.1016/0009-2509(94)E0086-6)
- Nguyễn T.T., Sederman A.J., Mantle M.D., Gladden L.F., Segregation in horizontal rotating cylinders using magnetic resonance imaging, *Physical Review E*, 84 (2011) 011304. <https://doi.org/10.1103/PhysRevE.84.011304>
- Nicușan A., Windows-Yule C., Positron emission particle tracking using machine learning, *Review of Scientific Instruments*, 91 (2020) 013329. <https://doi.org/10.1063/1.5129251>
- Parker D., Dijkstra A., Martin T., Seville J., Positron emission particle tracking studies of spherical particle motion in rotating drums, *Chemical Engineering Science*, 52 (1997) 2011–2022. [https://doi.org/10.1016/S0009-2509\(97\)00030-4](https://doi.org/10.1016/S0009-2509(97)00030-4)
- Parker J.T., DeBerardinis J., Mäkiharju S.A., Enhanced laboratory X-ray particle tracking velocimetry with newly developed tungsten-coated O (50 μm) tracers, *Experiments in Fluids*, 63 (2022) 184. <https://doi.org/10.1007/s00348-022-03530-6>
- Patil H., Patel A.K., Pant H.J., Vinod A.V., Numerical modelling of stirred tank and its validation by radioactive particle tracking (RPT) technique, *ISH Journal of Hydraulic Engineering*, 28 (2020) 327–340. <https://doi.org/10.1080/09715010.2020.1797543>
- Penn A., Boyce C.M., Conzelmann N., Bezing G., Pruessmann K.P., Müller C.R., Real-time magnetic resonance imaging of fluidized beds with internals, *Chemical Engineering Science*, 198 (2019) 117–123. <https://doi.org/10.1016/j.ces.2018.12.041>
- Penn A., Boyce C.M., Kovar T., Tsuji T., Pruessmann K.P., Müller C.R., Real-time magnetic resonance imaging of bubble behavior and particle velocity in fluidized beds, *Industrial & Engineering Chemistry Research*, 57 (2018) 9674–9682. <https://doi.org/10.1021/acs.iecr.8b00932>
- Penn A., Tsuji T., Brunner D.O., Boyce C.M., Pruessmann K.P., Müller C.R., Real-time probing of granular dynamics with magnetic resonance, *Science Advances*, 3 (2017) e1701879. <https://doi.org/10.1126/sciadv.1701879>
- Radman J.R., Langlois R., Leadbeater T., Finch J., Rowson N., Waters K., Particle flow visualization in quartz slurry inside a hydrocyclone using the positron emission particle tracking technique, *Minerals Engineering*, 62 (2014) 142–145. <https://doi.org/10.1016/j.mineng.2014.03.019>
- Rao S., Bhatia S., Khakhar D., Axial transport of granular solids in rotating cylinders. Part 2: Experiments in a non-flow system, *Powder Technology*, 67 (1991) 153–162. [https://doi.org/10.1016/0032-5910\(91\)80152-9](https://doi.org/10.1016/0032-5910(91)80152-9)
- Rasouli M., Bertrand F., Chaouki J., A multiple radioactive particle tracking technique to investigate particulate flows, *AIChE Journal*, 61 (2015) 384–394. <https://doi.org/10.1002/aic.14644>
- Richter M., Mainza A., Govender I., Mangadoddy N., Sivakumar R., Sreedhar G., van Heerden M., Features of near gravitational material tracers in a dense medium cyclone from PEPT, *Powder Technology*, 415 (2023) 118095. <https://doi.org/10.1016/j.powtec.2022.118095>
- Roy S., Larachi F., Al-Dahhan M., Duduković M., Optimal design of radioactive particle tracking experiments for flow mapping in opaque multiphase reactors, *Applied Radiation and Isotopes*, 56 (2002) 485–503. [https://doi.org/10.1016/S0969-8043\(01\)00142-7](https://doi.org/10.1016/S0969-8043(01)00142-7)
- Roy S., Pant H.J., Roy S., Velocity characterization of solids in binary fluidized beds, *Chemical Engineering Science*, 246 (2021) 116883. <https://doi.org/10.1016/j.ces.2021.116883>
- Roy S., Roy S., Modelling of binary fluidization of coal and ash and validation using radioactive particle tracking and densitometry, *The Canadian Journal of Chemical Engineering*, 101 (2023) 1660–1679. <https://doi.org/10.1002/cjce.24430>
- Saayman J., Nicol W., Van Ommen J.R., Mudde R.F., Fast X-ray tomography for the quantification of the bubbling-, turbulent- and fast fluidization-flow regimes and void structures, *Chemical Engineering Journal*, 234 (2013) 437–447. <https://doi.org/10.1016/j.ces.2013.09.008>
- Salerno G., Maestri M., Fraguio M.S., Picabea J., Cassanello M., De Blasio C., Cardona M.A., Hojman D., Somacal H., Study on the aggregate motion for gas–liquid–solid agitated tank reactors design using radioactive particle tracking, *Measurement Science and Technology*, 33 (2022) 094004. <https://doi.org/10.1088/1361-6501/ac73dd>
- Savari C., Li K., Barigou M., Comparative evaluation of electrical resistance tomography, positron emission particle tracking and high-speed imaging for analysing horizontal particle-liquid flow in a pipe, *Powder Technology*, 438 (2024) 119606. <https://doi.org/10.1016/j.powtec.2024.119606>
- Seeger A., Kertzscher U., Affeld K., Wellenhofer E., Measurement of the local velocity of the solid phase and the local solid hold-up in a three-phase flow by X-ray based particle tracking velocimetry (XPTV), *Chemical Engineering Science*, 58 (2003) 1721–1729. [https://doi.org/10.1016/S0009-2509\(03\)00010-1](https://doi.org/10.1016/S0009-2509(03)00010-1)
- Sovechles J., Boucher D., Pax R., Leadbeater T., Sasmito A., Waters K., Performance analysis of a new positron camera geometry for high speed, fine particle tracking, *Measurement Science and Technology*, 28 (2017) 095402. <https://doi.org/10.1088/1361-6501/aa7dce>

- Stannarius R., Magnetic resonance imaging of granular materials, *Review of Scientific Instruments*, 88 (2017) 051806.
<https://doi.org/10.1063/1.4983135>
- Stannarius R., Martinez D.S., Börzsönyi T., Bieberle M., Barthel F., Hampel U., High-speed X-ray tomography of silo discharge, *New Journal of Physics*, 21 (2019) 113054.
<https://doi.org/10.1088/1367-2630/ab5893>
- Stein M., Ding Y., Seville J., Parker D., Solids motion in bubbling gas fluidised beds, *Chemical Engineering Science*, 55 (2000) 5291–5300.
[https://doi.org/10.1016/S0009-2509\(00\)00177-9](https://doi.org/10.1016/S0009-2509(00)00177-9)
- Tribedi T., Pillajetti P., Kumari R., Pant H.J., Tiwari P., Upadhyay R.K., Measurements of solid velocity in a pilot-scale Geldart's group B circulating fluidized bed using a radioactive particle tracking technique, *Industrial & Engineering Chemistry Research*, 61 (2022) 9110–9121. <https://doi.org/10.1021/acs.iecr.2c01119>
- Tribedi T., Tiwari P., Pant H.J., Upadhyay R.K., Solid flow mapping at the bottom section of a pilot-plant scale riser with the help of a radioactive particle tracking technique, *Industrial & Engineering Chemistry Research*, 62 (2023) 19133–19144.
<https://doi.org/10.1021/acs.iecr.3c00788>
- Tupper G.B., Govender I., De Klerk D.N., Richter M.C., Mainza A.N., Testing of a new dynamic Ergun equation for transport with positron emission particle tracking, *AIChE Journal*, 62 (2016) 939–946.
<https://doi.org/10.1002/aic.15081>
- Uchida K., Okamoto K., Measurement of powder flow in a screw feeder by x-ray penetration image analysis, *Measurement Science and Technology*, 17 (2006) 419.
<https://doi.org/10.1088/0957-0233/17/2/025>
- Upadhyay R.K., Roy S., Investigation of hydrodynamics of binary fluidized beds via radioactive particle tracking and dual-source densitometry, *The Canadian Journal of Chemical Engineering*, 88 (2010) 601–610. <https://doi.org/10.1002/cjce.20334>
- Van der Sande P.C., Wagner E.C., de Mooij J., Meesters G.M., van Ommen J.R., Particle dynamics in horizontal stirred bed reactors characterized by single-photon emission radioactive particle tracking, *Chemical Engineering Journal*, 482 (2024) 149100.
<https://doi.org/10.1016/j.cej.2024.149100>
- Vesvikar M.S., Aljuwaya T.M., Taha M.M., Al-Dahhan M.H., Development, validation and implementation of multiple radioactive particle tracking technique, *Nuclear Engineering and Technology*, 55 (2023) 4213–4227. <https://doi.org/10.1016/j.net.2023.07.043>
- Vieira W.S., Brandão L.E.B., Braz D., An alternative method for tracking a radioactive particle inside a fluid, *Applied Radiation and Isotopes*, 85 (2014) 139–146. <https://doi.org/10.1016/j.apradiso.2013.12.006>
- Waktola S., Bieberle A., Barthel F., Bieberle M., Hampel U., Grudziński K., Babout L., A new data-processing approach to study particle motion using ultrafast X-ray tomography scanner: case study of gravitational mass flow, *Experiments in Fluids*, 59 (2018) 69.
<https://doi.org/10.1007/s00348-018-2523-2>
- Wiggins C., Santos R., Ruggles A., A novel clustering approach to positron emission particle tracking, *Nuclear Instruments and Methods in Physics Research Section A: Accelerators, Spectrometers, Detectors and Associated Equipment*, 811 (2016) 18–24.
<https://doi.org/10.1016/j.nima.2015.11.136>
- Wiggins C., Santos R., Ruggles A., A feature point identification method for positron emission particle tracking with multiple tracers, *Nuclear Instruments and Methods in Physics Research Section A: Accelerators, Spectrometers, Detectors and Associated Equipment*, 843 (2017) 22–28. <https://doi.org/10.1016/j.nima.2016.10.057>
- Wildman R., Huntley J., Stochastic aspects of granular flow in vibrated beds, *KONA Powder and Particle Journal*, 20 (2002) 105–114.
<https://doi.org/10.14356/kona.2002013>
- Windisch D., Bieberle M., Bieberle A., Hampel U., Control concepts for image-based structure tracking with ultrafast electron beam X-ray tomography, *Transactions of the Institute of Measurement and Control*, 42 (2020) 691–703. <https://doi.org/10.1177/0142331219858048>
- Windows-Yule C., Herald M., Nicușan A., Wiggins C., Pratz G., Manger S., Odo A., Leadbeater T., Pellico J., de Rosales R.T., Recent advances in positron emission particle tracking: a comparative review, *Reports on Progress in Physics*, 85 (2022) 016101.
<https://doi.org/10.1088/1361-6633/ac3c4c>
- Windows-Yule C., Scheper B., Van Der Horn A., Hainsworth N., Saunders J., Parker D., Thornton A., Understanding and exploiting competing segregation mechanisms in horizontally rotated granular media, *New Journal of Physics*, 18 (2016) 023013.
<https://doi.org/10.1088/1367-2630/18/2/023013>
- Windows-Yule C., Van Der Horn A., Tunuguntla D., Parker D., Thornton A., Inducing axial banding in bidisperse-by-density granular systems using noncylindrical tumbler geometries, *Physical Review Applied*, 8 (2017) 024010. <https://doi.org/10.1103/PhysRevApplied.8.024010>
- Windows-Yule C.R., Hart-Villamil R., Ridout T., Kokalova T., Nogueira-Filho J.C., Positron emission particle tracking for liquid-solid mixing in stirred tanks, *Chemical Engineering & Technology*, 43 (2020) 1939–1950. <https://doi.org/10.1002/ceat.202000177>
- Xi K., Guo Q., Boyce C.M., Comparison of two-fluid model simulations of freely bubbling three-dimensional gas-fluidized beds with magnetic resonance imaging results, *Industrial & Engineering Chemistry Research*, 60 (2021a) 7429–7442.
<https://doi.org/10.1021/acs.iecr.1c00050>
- Xi K., Kovar T., Fullmer W.D., Penn A., Musser J., Boyce C.M., CFD-DEM study of bubble properties in a cylindrical fluidized bed of Geldart Group D particles and comparison with prior MRI data, *Powder Technology*, 389 (2021b) 75–84.
<https://doi.org/10.1016/j.powtec.2021.04.075>
- Yadav A., Gaurav T.K., Pant H.J., Roy S., Machine learning based position-rendering algorithms for radioactive particle tracking experimentation, *AIChE Journal*, 66 (2020a) e16954.
<https://doi.org/10.1002/aic.16954>
- Yadav A., Pant H.J., Roy S., Velocity measurements in convective boiling flow using radioactive particle tracking technique, *AIChE Journal*, 66 (2020b) e16782. <https://doi.org/10.1002/aic.16782>
- Yadav A., Ramteke M., Pant H.J., Roy S., Monte Carlo real coded genetic algorithm (MC-RGA) for radioactive particle tracking (RPT) experimentation, *AIChE Journal*, 63 (2017) 2850–2863.
<https://doi.org/10.1002/aic.15596>
- Yang C.Y., Fu X.Y., Development and validation of a material-labeling method for powder process characterization using X-ray computed tomography, *Powder Technology*, 146 (2004) 10–19.
<https://doi.org/10.1016/j.powtec.2004.06.011>
- Yang Z., Fryer P., Bakalis S., Fan X., Parker D., Seville J., An improved algorithm for tracking multiple, freely moving particles in a positron emission particle tracking system, *Nuclear Instruments and Methods in Physics Research Section A: Accelerators, Spectrometers, Detectors and Associated Equipment*, 577 (2007) 585–594.
<https://doi.org/10.1016/j.nima.2007.01.089>
- Yang Z., Parker D., Fryer P., Bakalis S., Fan X., Multiple-particle tracking—an improvement for positron particle tracking, *Nuclear Instruments and Methods in Physics Research Section A: Accelerators, Spectrometers, Detectors and Associated Equipment*, 564 (2006) 332–338. <https://doi.org/10.1016/j.nima.2006.04.054>
- Yates J., Cheesman D., Lettieri P., Newton D., X-ray analysis of fluidized beds and other multiphase systems, *KONA Powder and Particle Journal*, 20 (2002) 133–143. <https://doi.org/10.14356/kona.2002016>
- Yunos M.A.S.M., Hussain S.A., Yusoff H.M., Abdullah J., Preparation and quantification of radioactive particles for tracking hydrodynamic behavior in multiphase reactors, *Applied Radiation and Isotopes*, 91 (2014) 57–61. <https://doi.org/10.1016/j.apradiso.2014.05.015>
- Zhou M., Kökkılıç O., Boucher D., Lepage M., Leadbeater T.W., Langlois R., Waters K.E., Investigation of particle motion in a dry separation fluidized bed using PEPT, *Minerals*, 13 (2023) 254.
<https://doi.org/10.3390/min13020254>
- Zhou X., Dai N., Cheng X., Thompson A., Leach R., Three-dimensional characterization of powder particles using X-ray computed tomography, *Additive Manufacturing*, 40 (2021) 101913.
<https://doi.org/10.1016/j.addma.2021.101913>
- Zhu A., Mao C., Luner P.E., Lomeo J., So C., Marchal S., Zhang S., Investigation of quantitative X-ray microscopy for assessment of API and excipient microstructure evolution in solid dosage processing, *AAPS PharmSciTech*, 23 (2022) 117.
<https://doi.org/10.1208/s12249-022-02271-3>

Authors' Short Biographies



Dr. Tsuo-Feng Wang received her BS degree in Department of Chemical Engineering, National Taiwan University, Taiwan in 1995 and Ph.D. degree in Department of Chemical and Biological Engineering, University at Buffalo, USA in 2003. She is currently Postdoctoral Research Fellow at Department of Chemical Engineering, National Taiwan University, Taiwan. Her main research interest is in the transport phenomena occurring in bio-materials and chemical engineering processes.



Dr. An-Ni Huang received her Ph.D. degree in Chemical and Materials Engineering from Chang Gung University, Taiwan in 2012. After working at Hiroshima University as an Assistant Professor, she joined Chang Gung University in 2017 and is currently Associate Professor at the same university. She is Editor of Advanced Powder Technology Journal. Her research interests include CFD-DEM modeling of multiphase flows, mixing and improvement of unit operations.



Ms. Wan-Yi Hsu received her master degree in Department of Chemical and Materials Engineering, Chang Gung University, Taiwan in 2016. She is currently Associate Assistant Research Fellow at Green Technology Research Center, Chang Gung University, Taiwan. Her research interests include modeling of multiphase flows and fluidization related applications.



Prof. Hsiu-Po Kuo received his B.Sc. degree and Ph.D. degree in Chemical Engineering from National Taiwan University, Taiwan in 1995 and from the University of Birmingham, UK in 2001, respectively. He joined Chang Gung University in 2002 and promoted as full Professor in 2012. He moved to National Taiwan University in 2020. He is interested in particle technology related studies. He was the most-contributed Editor, Associate Executive Editor and Executive Editor of Advanced Powder Technology Journal. He works closely with the several industrial partners in Taiwan.